# Interstellar Medium (ISM)

## Lecture 14
## 2025 June 02 (Monday), 9AM

updated 03/03, 23:23

선광일 (Kwangil Seon)
KASI / UST

# [Hyperfine Splitting & Ortho-$H_2$ and Para-$H_2$]

- **Hyperfine splitting:** If one or more nuclei have nonzero nuclear spin and $J_{ez} \neq 0$, then there will be an interaction between the nuclear magnetic moment and the magnetic field generated by the electrons, resulting in "hyperfine splitting." The energy will depend on the orientation of the nuclear angular momentum relative to the axis.

- **Ortho-$H_2$ and Para-$H_2$ (spin isomers, 이상질체)**

  In the case of $H_2$, the electronic wave function is required to be antisymmetric under exchange of the two electrons.

  The two protons, just like electrons, are identical fermions, and therefore, the Pauli exclusion principle antisymmetric requirement also applies to **exchange of the two protons**. The protons are spin 1/2 particles - the two protons together can have total spin 1 (parallel) or total spin 0 (antiparallel).

  The consequence of the antisymmetry requirement is that

  If the protons have spin 0, the rotational quantum number $J$ must be even. $\Rightarrow$ para-$H_2$ (even $J$)
  (an antisymmetric nuclear spin wave function ($I = 0$) and a symmetric spatial wave function having an even value of the rotational quantum number $J$)
  If the protons have spin 1, the rotational quantum number $J$ must be odd. $\Rightarrow$ ortho-$H_2$ (odd $J$)
  (a symmetric nuclear spin wave function ($I = 1$) and an antisymmetric spatial wave function having an odd value of the rotational quantum number $J$)

  Because the nuclear spins are only weakly coupled to the electromagnetic field, **ortho-$H_2$ and para-$H_2$ behave as almost distinct species.**

## H$_2$ has no permanent electric dipole moment.

- Thus, the vibrational states and the rotational states radiate very weakly, via the time-variation of the electric quadrupole moment and the molecule vibrates or rotates.

- Because the nuclear spin state does not change, the ro-vibrational radiative transitions of H$_2$ must have

$$\Delta J = 0 \text{ or } \Delta J = \pm 2, \text{ i.e., ortho } \rightarrow \text{ ortho or para } \rightarrow \text{ para}$$
$$(\text{not } J = 0 \leftrightarrow J = 0)$$

The vibration-rotation emission spectrum of H$_2$ therefore consists of electric quadrupole transitions. Therefore, the H$_2$ emission lines are faint and hard to detect. The downward transitions are identified by

$$v_u - v_\ell \ \text{S}(J_\ell) \quad \text{if } J_\ell = J_u - 2 \quad ,$$
$$v_u - v_\ell \ \text{Q}(J_\ell) \quad \text{if } J_\ell = J_u \quad ,$$
$$v_u - v_\ell \ \text{O}(J_\ell) \quad \text{if } J_\ell = J_u + 2 \quad .$$

For example, 1-0 S(1) refers to the transition $(v = 1, \ J = 3) \rightarrow (v = 0, \ J = 1)$.

the next Figure.

- Spin-exchange collisions with H$^0$ or H$^+$, and a process in which H$_2$ is captured on a grain surface, can cause an ortho-para conversion.

- The statistical weight of an ortho-H$_2$ rotational level $J$ is $3(2J+1)$ [because $S_{\text{nucleus}} = 1$].

For a para-H$_2$ it is $(2J+1)$ [because $S_{\text{nucleus}} = 0$].

# Ortho/Para Ratios

- The ortho state of a molecule is defined as having the larger statistical spin weights and para as having the smaller weight.

- Since the typical energy separation between the ortho and para states of a molecule is comparable to the gas and dust temperature in the ISM and much smaller than the energy released in formation reactions, **it is expected that the abundance ratio between the two states will reflect the equilibrium values at high temperatures, that is, the ratio of their statistical weight.**

$$\frac{E_{J=1} - E_{J=0}}{k_{\mathrm{B}}} \approx 174.98 \, \mathrm{K} \quad \text{for H}_2$$

  ‣ Since g = 2I + 1, the usual ortho to para ratio is (2x1+1)/(2x0+1) = 3 for spin 1/2 systems such as $H_2$.

- If a molecule cannot be converted from ortho to para (or vice versa) by radiative or collisional processes, the two states can effectively be considered as two separate molecules. In this case, the ortho to para ratio at the time of molecule formation will be preserved.

# Interstellar Molecules

- Interstellar Molecules

  - Interstellar molecules were first discovered in the late 1930s through the identification of optical lines seen in absorption against background starlight with electronic transitions of molecules.

  - The molecules first detected were CN ($B^2\Sigma^+ - X^2\Sigma^+$ at 3876.84Å), CH ($A^2\Delta - X^2\Pi$ at 4300.30Å) and CH$^+$ ($A^1\Pi - X^1\Pi^+$ at 4232.54Å)

  - To date, over 200 interstellar molecules have been detected.

Interstellar molecules listed by number of atoms

| Diatomic | Triatomic | Four atoms | Five atoms | Six atoms | Seven atoms | Eight atoms |
|---|---|---|---|---|---|---|
| $H_2$ | $C_3$ | $c$-$C_3H$ | $C_5$ | $C_5H$ | $C_6H$ | $CH_3C_3N$ |
| AlF | $C_2H$ | $l$-$C_3H$ | $C_4H$ | $l$-$H_2C_4$ | $CH_2CHCN$ | $HCOOCH_3$ |
| AlCl | $C_2O$ | $C_3N$ | $C_4Si$ | $C_2H_4$ | $CH_3C_2H$ | $CH_3COOH(?)$ |
| $C_2$ | $C_2S$ | $C_3O$ | $l$-$C_3H_2$ | $CH_3CN$ | $HC_5N$ | $C_7H$ |
| CH | $CH_2$ | $C_3S$ | $c$-$C_3H_2$ | $CH_3NC$ | $HCOCH_3$ | $H_2C_6$ |
| CH$^+$ | HCN | $C_2H_2$ | $CH_2CN$ | $CH_3OH$ | $NH_2CH_3$ | $CH_2OHCHO$ |
| CN | HCO | $CH_2D^+(?)$ | $CH_4$ | $CH_3SH$ | $c$-$C_2H_4O$ | $CH_2CHCHO$ |
| CO | HCO$^+$ | HCCN | $HC_3N$ | $HC_3NH^+$ | $CH_2CHOH$ | |
| CO$^+$ | HCS$^+$ | HCNH$^+$ | $HC_2NC$ | $HC_2CHO$ | | |
| CP | HOC$^+$ | HNCO | HCOOH | $NH_2CHO$ | | |
| CSi | $H_2O$ | HNCS | $H_2CHN$ | $C_5N$ | | |
| HCl | $H_2S$ | HOCO$^+$ | $H_2C_2O$ | $HC_4N$ | | |
| KCl | HNC | $H_2CO$ | $H_2NCN$ | | | |
| NH | HNO | $H_2CN$ | $HNC_3$ | | | |
| NO | MgCN | $H_2CS$ | $SiH_4$ | | | |
| NS | MgNC | $H_3O^+$ | $H_2COH^+$ | | | |
| NaCl | $N_2H^+$ | $NH_3$ | | | | |
| OH | $N_2O$ | $SiC_3$ | | | | |
| PN | NaCN | $C_4$ | | | | |
| SO | OCS | | | | | |
| SO$^+$ | $SO_2$ | | | | | |
| SiN | $c$-$SiC_2$ | | | | | |
| SiO | $CO_2$ | | | | | |
| SiS | $NH_2$ | | | | | |
| CS | $H_3^+$ | | | | | |
| HF | SiCN | | | | | |
| SH | AlNC | | | | | |
| FeO(?) | SiNC | | | | | |

| Nine atoms | Ten atoms | Eleven atoms | Twelve atoms | Thirteen atoms |
|---|---|---|---|---|
| $CH_3C_4H$ | $CH_3C_5N(?)$ | $HC_9N$ | $CH_3OC_2H_5$ | $HC_{11}N$ |
| $CH_3CH_2CN$ | $(CH_3)_2CO$ | | | |
| $(CH_3)_2O$ | $NH_2CH_2COOH$ | | | |
| $CH_3CH_2OH$ | $CH_3CH_2CHO$ | | | |
| $HC_7N$ | | | | |
| $C_8H$ | | | | |

Table from A. Wootten (www.cv.nrao.edu/~awootten/allmols.html).

[Table 7.1, Kowk]

- Given the ubiquity of hydrogen in the ISM, and the inability of helium to form chemical bonds, we expect molecular gas in the ISM to consist primarily of $H_2$.

  - A hydrogen molecule, with the dissociation energy $D_0 = 4.52$ eV, is not very tightly bound. An UV photon can photodissociate it.

  - In a gas with temperature $T > D_0/k \sim 50{,}000$ K , collisions with other gas particles can collisionally dissociate it. Thus, we expect molecular hydrogen to survive for long periods of time **only in cold regions of the ISM that are shielded from UV radiation.**

  - Hydrogen has the lowest, reduced mass of any molecule, $\mu = m_H/2$, hence, hydrogen molecules have a particularly high fundamental frequency of vibration compared to other diatomic molecules.

Properties of some diatomic molecules [Table 7.1, Ryden]

| Molecule | $D_0$ [eV] | $r_0$ Å | $B_0$ [meV] | $\hbar\omega_0$ [eV] | $\mu_0$ [debye] |
|---|---|---|---|---|---|
| $H_2$ | 4.52 | 0.74 | 7.36 | 0.516 | 0.000 |
| CO | 11.1 | 1.13 | 0.24 | 0.269 | 0.110 |
| CH | 3.51 | 1.12 | 1.76 | 0.339 | 1.406 |
| OH | 4.39 | 0.97 | 2.30 | 0.443 | 1.668 |
| CN | 7.57 | 1.17 | 0.23 | 0.253 | 0.557 |

$\mu_0 =$ permanent dipole moment

1 debye $= 10^{-18}$ statC cm

$D_0 =$ dissociation energy

$r_0 =$ speration

$B_0 \equiv \dfrac{\hbar^2}{2I}$

$\omega_0 = \sqrt{k/\mu}$ fundamental frequency of vibration

# CO

- For any molecule to undergo a pure rotation transition, it must have a permanent dipole moment, $\mu$. This means that **for any molecule to have a dipole-allowed rotational spectrum it must have an asymmetric charge distribution which gives rise to a permanent dipole moment.**

  Heteronuclear diatomics poses a permanent dipole moment but homonuclears, such as $H_2$, do not.

- CO

  Carbon monoxide, CO, is a particularly important species for astronomical observations.

  **CO is the most stable diatomic molecule.**

  It has a dissociation energy $D_0$ of 11.1 eV, which is more than double the $D_0$ value found for most other diatomic molecules. As a result, in astronomical environments where molecules form, C and O usually combine to form CO, which is very stable and long-lived.

  The wavelengths of the first few rotational transitions are 1-0 at $\lambda = 2.60$ mm, 2-1 at 1.30 mm, and 3-2 at 0.87mm.

  **The J = 1-0 transition of CO is the second most important spectral line in radio astronomy after the hydrogen 21 cm line.**

CO is widely distributed in the interstellar medium and maps of the CO J = 1-0 transition are a standard tool for investigating the ISM.

One reason for this is that cold $H_2$ is very difficult to observe directly because its pure rotational transitions are not only very weak but lie in the near-infrared where ground-based observations are not possible. **The abundance of CO is therefore often used to estimate the total amount of molecular gas present in a given environment.** It is generally assumed that the number density of CO is approximately $10^{-4}$ of that of $H_2$.

$$n(\mathrm{CO}) \approx 10^{-4} n(\mathrm{H_2})$$

If, as often happens, the CO 1-0 line is optically thick, one can use higher transitions such as the CO 2-1 line instead. Another option to avoid the effects of optical thickness is to observe an isotopologue $^{13}\mathrm{CO}$, which is present with much lower densities and whose transitions are therefore much less optically thick.

An isotopologue is a molecule that consists of at least one less abundant isotope of its constituent elements. They have the same transitions at nearby frequencies with similar decay and excitation rates. The main difference is in their abundance and observations of the rarer species help diagnose conditions in dense regions where lines from the primary species are optically thick.
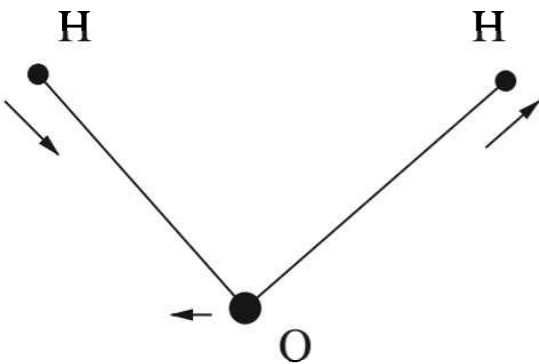
# Vibrations in Polyatomic Molecules

$H_2O$
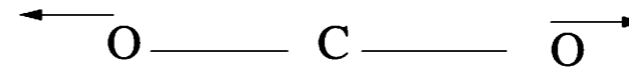
$CO_2$
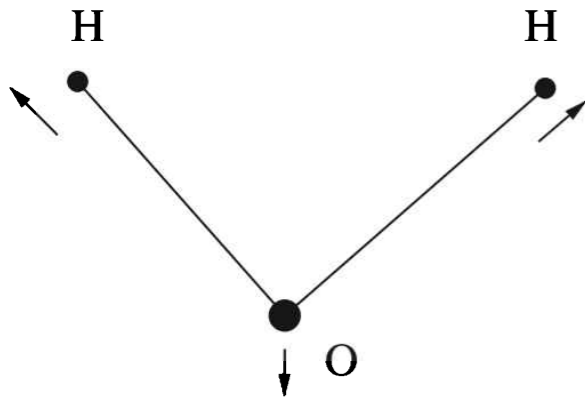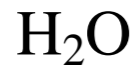
Symmetric stretch, $\nu_1$

$\omega_1 = 3667$ cm$^{-1}$

O —— C —— O    Symmetric stretch, $\nu_1$

$\omega_1 = 1388$ cm$^{-1}$

Bend, $\nu_2$

$\omega_2 = 1595$ cm$^{-1}$
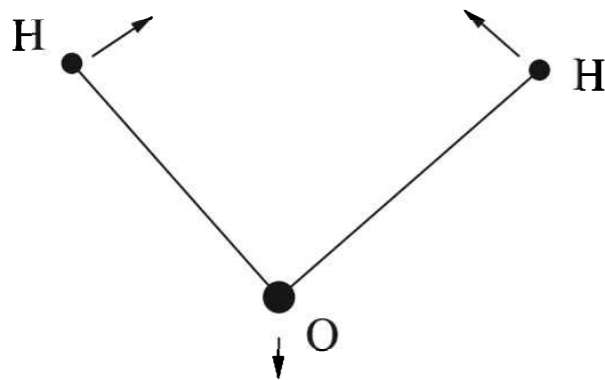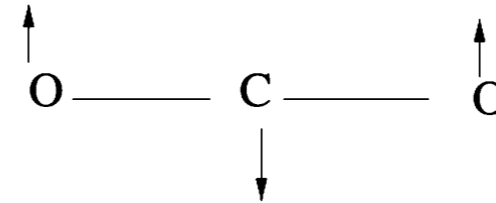
O —— C —— O    Bend (degenerate), $\nu_2$

$\omega_2 = 667$ cm$^{-1}$

Asymmetric stretch, $\nu_3$

$\omega_3 = 3676$ cm$^{-1}$
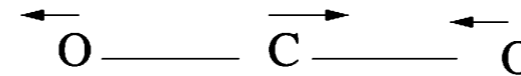
O —— C —— O    Asymmetric stretch, $\nu_3$

$\omega_3 = 2349$ cm$^{-1}$

The three vibrational modes of the **water molecule**

The vibrational modes of **carbon dioxide**; note that the bending mode is doubly degenerate as the motion can occur in the plane of the page, as drawn, or identically, perpendicular to the plane of the page.

# [H₂ formation] (1) Gas-Phase Formation of H₂

- **Direct Radiative Association**

  - When two free H atoms collide with each other, they create an excited hydrogen molecule that is unbound.

$$\mathrm{H} + \mathrm{H} \rightarrow \mathrm{H}_2^* \rightarrow \mathrm{H}_2 + h\nu$$
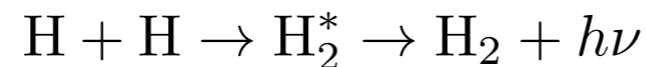
  - It must emit a photon carrying away enough energy to leave it a bound state, or it will break apart again. There is no electric dipole moment. As a result, there is no dipole radiation that could remove energy from the system and leave the two H atoms in a bound state. Electric quadrupole transitions are possible, but the rates are very low.

    The lifetime of the excited hydrogen molecule until it breaks apart would be roughly one period of vibration:
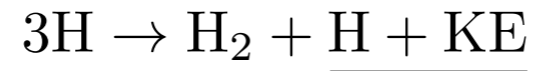
$$\frac{2\pi}{\omega_0} = \frac{h}{E_{\mathrm{vib},0}} = \frac{6.626 \times 10^{-27}\,\mathrm{cm^2\,g\,s^{-1}}}{0.516\,\mathrm{eV}} \sim 8 \times 10^{-15}\,\mathrm{s}$$

    Rate for the electric quadrupole transition is $\quad A_{u\ell} \sim 10^{-11}\,\mathrm{s}^{-1}$

    Therefore, the probability of emitting a photon before it break apart is $\boxed{p \sim A_{u\ell}\,(2\pi/\omega_0) \sim 10^{-25}}$

  - As a consequence, the rate coefficient for direct radiative association of H₂ is so small that this reaction can be ignored in astrochemistry.
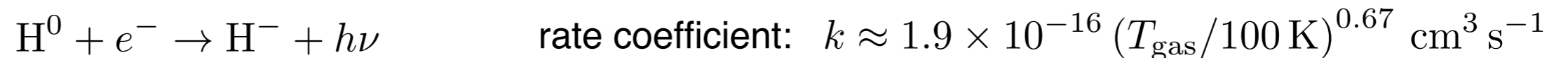
- **Three-body reaction**

$$3\mathrm{H} \rightarrow \mathrm{H}_2 + \underline{\mathrm{H} + \mathrm{KE}}$$

  - The reaction can occur, when the third body carrying off the energy released when $\mathrm{H}_2$ is formed, but the rate for this three-body reaction is negligible at interstellar or intergalactic densities.

  - At the high densities of a protostar or protoplanetary disk, the three-body reaction is able to convert H to $\mathrm{H}_2$.

- **Formation of negative hydrogen ion by radiative association followed by formation of $H_2$ by associative detachment**:

  - First step:

$$\mathrm{H}^0 + e^- \rightarrow \mathrm{H}^- + h\nu \qquad \text{rate coefficient:} \quad k \approx 1.9 \times 10^{-16}\,(T_{\mathrm{gas}}/100\,\mathrm{K})^{0.67}\ \mathrm{cm}^3\,\mathrm{s}^{-1}$$

  - Second step:

$$\mathrm{H}^- + \mathrm{H} \rightarrow \mathrm{H}_2 + e^- + \mathrm{KE} \qquad \text{rate coefficient:}\ k \approx 1.3 \times 10^{-9}\ \mathrm{cm}^3\,\mathrm{s}^{-1}$$

    This is an exothermic ion-molecule reaction.

  - The density of negative H ion is very low because the formation rate of $\mathrm{H}^-$ (first step) is slow while there are many, rapid processes that destroy $\mathrm{H}^-$.

▸ $H^-$ can be destroyed by reaction with protons:

$$H^- + H^+ \to H + H \qquad\qquad k \approx 6.9 \times 10^{-7} \, (T/100\,\mathrm{K})^{-1/2} \, \mathrm{cm^3 \, s^{-1}}$$
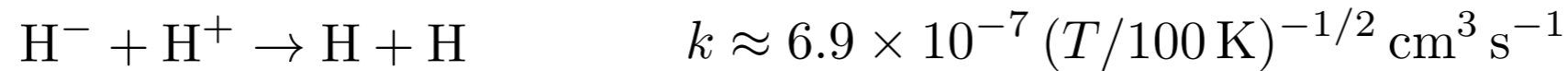
▸ $H^-$ can be destroyed by reaction with other positive ions:

$$H^- + X^+ \to H + X \qquad\qquad k \approx 4 \times 10^{-7} \, (T/100\,\mathrm{K})^{-1/2} \, \mathrm{cm^3 \, s^{-1}}$$

▸ In the diffuse ISM, $n(H^+) \approx 0.01\,\mathrm{cm^{-3}}$ or lower. Most of $H^-$ is destroyed by **photodetachment**, which is the inverse process to radiative association.

$$H^- + h\nu \to H + e^-$$

reaction rate: $\quad \zeta \approx 2.4 \times 10^{-7} G_0 \, \mathrm{s^{-1}}$

Here, $G_0$ is the strength of radiation in units of the interstellar radiation field (ISRF).

The photodetachment needs only $I = 0.77\,\mathrm{eV}$ to take away one of its electrons.

- ***In the absence of dust (e.g., in the early universe),*** $H^- + H \to H_2 + e^-$ ***is the dominant channel for forming H₂.***

▸ Associative detachment and the resulting production of H₂ will only dominate over photodetachment when

$$n_{\mathrm{HI}} > \frac{\zeta_{\mathrm{pd}}}{k_{\mathrm{ad}}} \approx 120\,\mathrm{cm^{-3}}$$
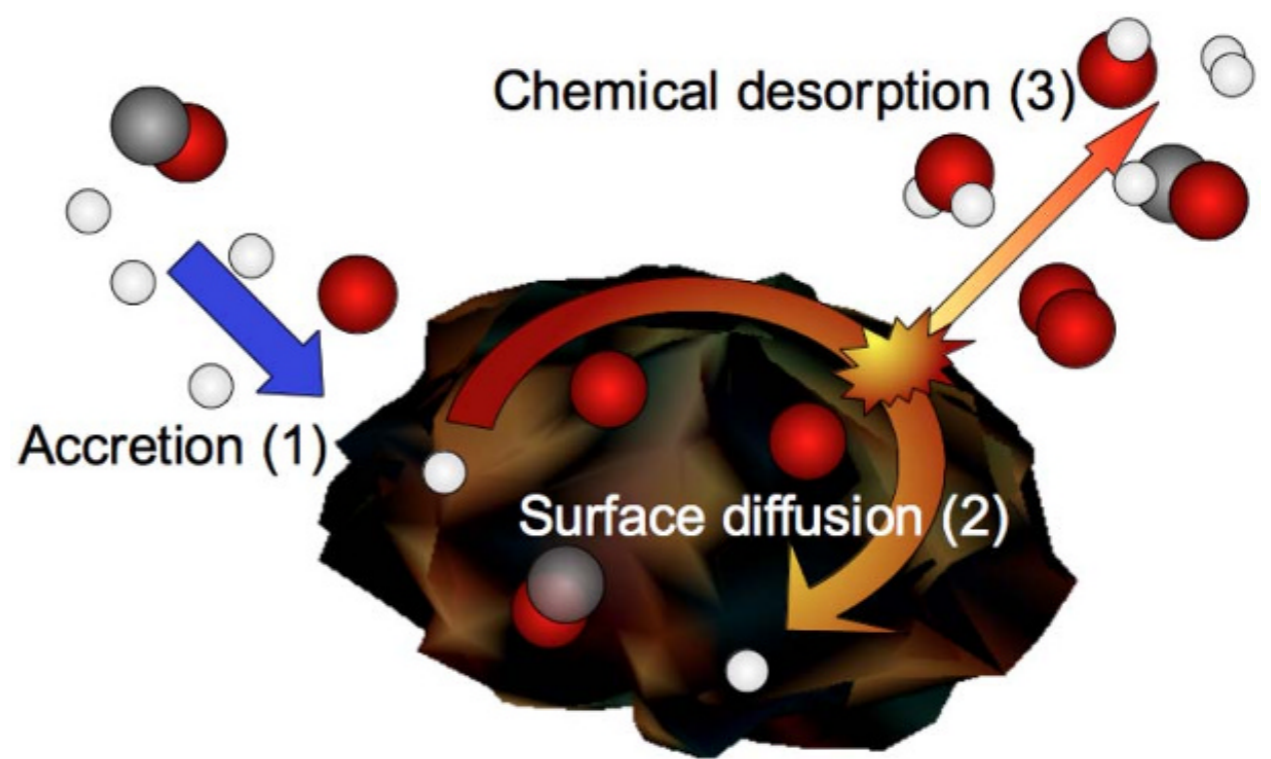
# [H₂ formation] (2) Grain Catalysis of H₂

- The dominant process of $H_2$ formation in the Milky Way and other galaxies is via grain catalysis.

  - The surface of a dust grain acts as a lab of chemical activity.

  - ***Adsorption***:

    ‣ A H atom colliding with a dust grain has some probability of sticking (bounding) to the grain.

    ‣ The sticking probability depends (1) on the atom's speed (slower atoms are more likely to stick), (2) on the grain's temperature (hot grains are less sticky), (3) on the grain's size (smaller grains are less sticky), and (4) on the grain's composition.

    ‣ Sticking probability: $\boxed{p_s \approx 0.3 \;\; \text{for grains with } a \sim 0.1 \mu\text{m}}$

  - ***Diffusion & Reaction***:

    ‣ Initially, the binding may be weak enough that the H atom is able to diffuse (i.e., random-walk) some distance on the grain surface, until it happens to arrive at a site where it is bound strongly enough that it becomes "trapped."

    ‣ Subsequent H atoms arrive at random locations on the grain surface and undergoes their own random walks until they also become trapped, but eventually one of the newly arrived H atoms encounters a previously bound H atom before itself becoming trapped.

    ‣ When the two H atoms encounter one another, they react to form $H_2$.

  - ***Desorption***:

    ‣ The energy released when two free H atoms react to form $H_2$ in the ground state is $\Delta E$ = 4.5 eV. This energy is large enough to overcome the forces that were binding the two H atoms to the grain, and the $H_2$ molecule is ejected from the grain surface.

ACCRETION

DIFFUSION

REACTION

EJECTION
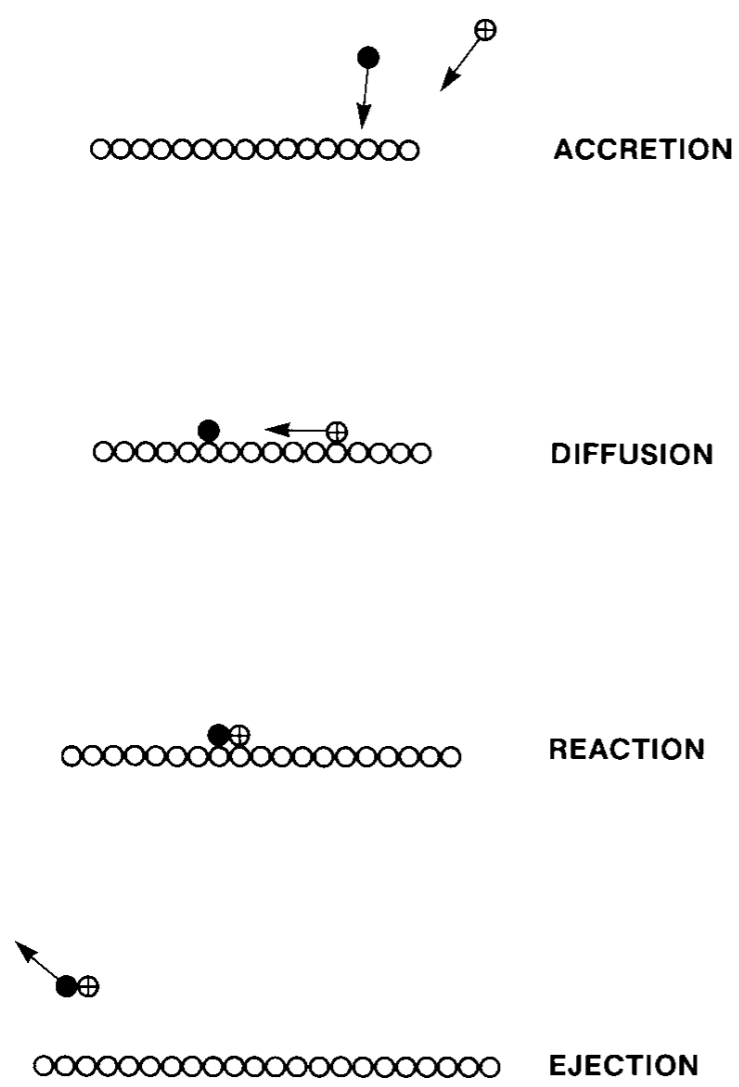
A schematic of the formation of molecules on grain surfaces.

[Fig 4.1, Tielens]



Chemical desorption (3)

Accretion (1)

Surface diffusion (2)

Sketch that illustrates the chemical desorption process. Species coming from the gas accrete on the dust surface can meet each other to form other species. For some reactions, the formed product is ejected in the gas.

[Fig 1, Dulieu, 2003, Scietific Reports]

# Formation rate of H$_2$

- Formation rate

  ▸ The rate per unit volume at which H atoms collide with grains, averaged over the distribution of grain radii would be:

  $$\Gamma_{\text{coll}} = n_{\text{HI}} \left( \frac{8kT_{\text{gas}}}{\pi m_{\text{H}}} \right)^{1/2} \int_{a_{\min}}^{a_{\max}} \frac{dn_{\text{gr}}}{da} \pi a^2 da$$

  > Recall the mean speed of the Maxwell distribution
  >
  > $$\langle v \rangle = \int_0^\infty v f(v) d^3 v = \sqrt{\frac{8kT}{\pi m}}$$
  >
  > $$f(v) = \left( \frac{m}{2\pi kT} \right)^{3/2} e^{-mv^2/2kT}$$

  ▸ It is customary to define *the total grain geometric cross section per H nucleon*.

  $$\Sigma_{\text{gr}} \equiv \frac{1}{n_{\text{H}}} \int da \frac{dn_{\text{gr}}}{da} \pi a^2 \quad \longrightarrow \quad \boxed{\Gamma_{\text{coll}} = n_{\text{HI}} n_{\text{H}} \left( \frac{8kT_{\text{gas}}}{\pi m_{\text{H}}} \right)^{1/2} \Sigma_{\text{gr}}}$$

  ▸ Suppose that a fraction $\epsilon_{\text{gr}}$ of the H atoms that collide with a grain depart from the grain as H$_2$. The rate for H$_2$ formation via grain catalysis would then be

  $$\frac{dn(\text{H}_2)}{dt} = \frac{1}{2} n_{\text{HI}} n_{\text{H}} \left( \frac{8kT_{\text{gas}}}{\pi m_{\text{H}}} \right)^{1/2} \int da \frac{dn_{\text{gr}}}{da} \pi a^2 \epsilon_{\text{gr}}(a)$$

  or   $$\frac{dn(\text{H}_2)}{dt} = R_{\text{gr}} n_{\text{H}} n_{\text{HI}}$$

  The factor 1/2 is because two H atoms are required to form H$_2$, and the **"rate coefficient"** is given by

  $$R_{\text{gr}} = \frac{1}{2} \left( \frac{8kT_{\text{gas}}}{\pi m_{\text{H}}} \right)^{1/2} \langle \epsilon_{\text{gr}} \rangle \Sigma_{\text{gr}}$$

  Here, the formation efficiency averaged over the grain surface area is:

  $$\langle \epsilon_{\text{gr}} \rangle \equiv \frac{1}{\Sigma_{\text{gr}}} \int da \frac{dn_{\text{gr}}}{da} \pi a^2 \epsilon_{\text{gr}}(a)$$

- Numerical values

  ▸ Total grain geometric cross section per H nucleon: We note that

  $$C(\lambda = 0.1\mu\mathrm{m}) \approx 2 \times 10^{-21}\,\mathrm{cm}^2/\mathrm{H} \quad \text{suggests that} \quad \Sigma_{\mathrm{gr}} \gtrsim 10^{-21}\,\mathrm{cm}^2/\mathrm{H}$$

  The silicate-graphite-PAH grain model of Weingartner & Draine (2001) gives

  $$\boxed{\Sigma_{\mathrm{gr}} \approx 6.0 \times 10^{-21}\,\mathrm{cm}^2/\mathrm{H}}$$

  ▸ The rate coefficient for H$_2$ formation is then

  $$\boxed{R_{\mathrm{gr}} = 7.3 \times 10^{-17}\,\mathrm{cm}^3\,\mathrm{s}^{-1} \left(\frac{T_{\mathrm{gas}}}{100\,\mathrm{K}}\right)^{1/2} \langle \epsilon_{\mathrm{gr}} \rangle \left(\frac{\Sigma_{\mathrm{gr}}}{10^{-21}\,\mathrm{cm}^2\,\mathrm{H}^{-1}}\right)}$$

  Jura (1975) used UV spectroscopy of diffuse clouds with $T_{\mathrm{gas}} \approx 70\,\mathrm{K}$ and determined that

  $$R_{\mathrm{gr}} \approx 3 \times 10^{-17}\,\mathrm{cm}^3\,\mathrm{s}^{-1}$$

  The observed rate coefficient indicates

  $$\boxed{\langle \epsilon_{\mathrm{gr}} \rangle \approx 0.08}$$

  This average is the result of a very low value of $\epsilon_{\mathrm{gr}}$ for the PAHs, which dominate the surface area, and $\boxed{\epsilon_{\mathrm{gr}} \gtrsim 0.5}$ for the $a \gtrsim 0.01\mu\mathrm{m}$ "classical" silicate and carbonaceous grains.

- Time scale of $H_2$ formation: dust grains are converting atomic hydrogen into molecular hydrogen on a characteristic time scale:

$$t_{\text{H}_2 \text{ form}} \approx \frac{\frac{1}{2} n_{\text{HI}}}{R_{\text{gr}} n_{\text{H}} n_{\text{HI}}}$$

$$\approx 15 \, \text{Myr} \left( \frac{n_{\text{H}}}{30 \, \text{cm}^{-3}} \right)^{-1} \left( \frac{T_{\text{gas}}}{100 \, \text{K}} \right)^{-1/2} \left( \frac{\langle \epsilon_{\text{gr}} \rangle}{0.08} \right)^{-1} \left( \frac{\Sigma_{\text{gr}}}{6 \times 10^{-21} \, \text{cm}^2 \, \text{H}^{-1}} \right)^{-1}$$

- Thus, **the CNM should be filled with molecular hydrogen** - unless there's a competing process that before the $H_2$ molecules as fast as grain surface make them.

- *The competing process is the photodissociation near bright stars.*

# Photodissociation of H$_2$

- ## Photodissociation: $H_2 + h\nu \rightarrow H + H + KE$

  - Photodissociation is the principal process destroying interstellar H$_2$.



Schematic drawing of the potential energy curves of molecular hydrogen [Figure 7.4, Ryden]
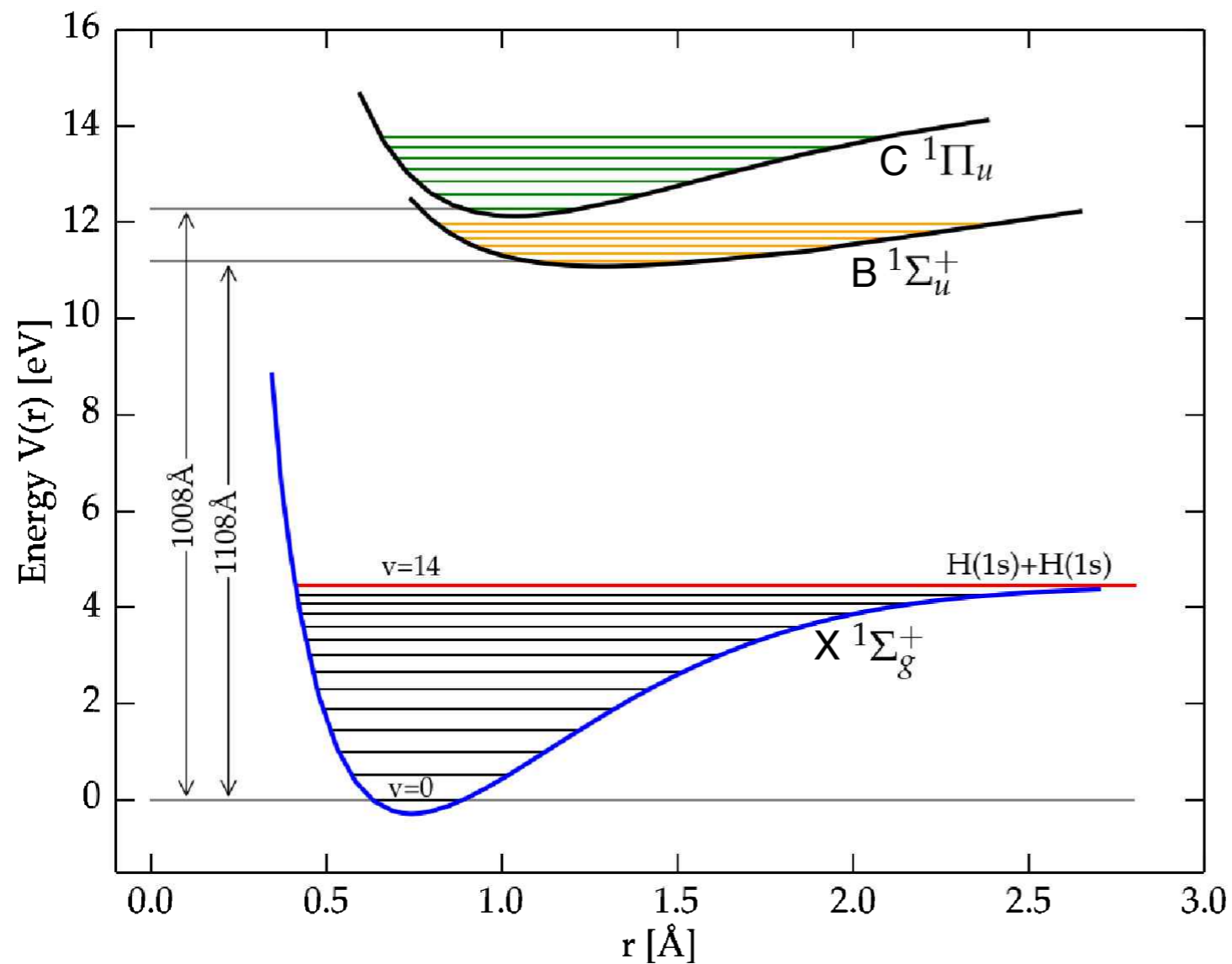
In the left potential energy curves, you might think that photodissociation of H$_2$ is a simple task; if H$_2$ absorb a photon of energy $h\nu > 4.52\,\text{eV}$, it will be excited to a vibrational state *(vibrational continuum)* with quantum number $v > 14$, which will be unbound.

However, absorbing a photon to lift the molecule to a $v > 14$ vibrational state requires a quadrupole transition, which has a very small transition probability.

- **Lyman-Werner band**

  ▸ The energy difference between the $v = 0, J = 0$ level in the ground electronic state, and the $v = 0, J = 0$ level in the first excited electronic state is $E = 11.18\,\text{eV}\ (\lambda = 1108\,\text{Å})$, which is a higher energy than the 10.2 eV energy of the Lyα line in atomic hydrogen.

  ▸ The transitions between the ro-vibrational levels in the ground electronic state and the ro-vibrational levels in the **first excited electronic states** produce a forest of lines that are referred to collectively as the *Lyman band*.

  ▸ Emission and absorption between the ground electronic state and the **second excited electronic state** is called the *Werner band*.

  ▸ The Lyman and Werner bands lie in the energy range 11.18 - 13.60 eV.

- The main mechanism by which H$_2$ is photodissociated is a two-step process.

  ▸ The first step is absorption of a resonance line photon (λ = 912-1108Å), raising the H$_2$ from an initial level $X(v, J)$ to a level $B(v', J')$ or $C(v', J')$ of the first and second electronic states. This photoexcitation is via a permitted absorption line, and therefore the newly excited level is guaranteed to have electric dipole-allowed decay channels, with a large transition probability.

  ▸ The excited level is most likely to decay to vibrationally excited bound levels $X(v'', J'')$ of the ground electronic state, and such decays occur ~85% of the time. However, a fraction of ~15% of the time, the downward spontaneous transition will be to the vibrational continuum ($v > 14$) of the ground electronic state: The two hydrogen atoms will then fly away from each other and the hydrogen molecule is dissociated.

- Photodissociation Rate:

  ▸ The probability per unit time of photoexcitation of H$_2$ from lower level $\ell$ to upper level $u$ is given by

  $$\zeta_{\ell \to u} = \frac{\pi e^2}{m_e c} f_{\ell u} \frac{u_\nu c}{h \nu_{\ell u}} \qquad \to \qquad \frac{\pi e^2}{m_e c^2 h} f_{\ell u} \lambda_{\ell u}^3 u_\lambda$$

  Eq (31.12) in Draine

  ▸ There are many transitions out of a given lower vibration-rotation level. The total rate of photoexcitation out of $\ell$ is:

  $$\zeta_{\mathrm{pe},\ell} = \sum_u \zeta_{\ell \to u}$$

  ▸ The photodissociation rate is obtained by summing over all of the photoexcitation channels, each multiplied by the probability $p_{\mathrm{diss},u}$ that the upper level will decay to the vibrational continuum:

  $$\zeta_{\mathrm{diss},\ell} = \sum_u \zeta_{\ell \to u} p_{\mathrm{diss},u}$$

  ▸ The dissociation probability averaged over the photoexcitation channels is:

  $$\langle p_{\mathrm{diss}} \rangle_\ell \equiv \frac{\zeta_{\mathrm{diss},\ell}}{\zeta_{\mathrm{pe},\ell}}$$

▸ Note that the photoexcitation and photodissociation rates are nearly independent of the level $\ell$.

| level $\ell$ $(v, J)$ | $\zeta_{\mathrm{photoexc},\ell}/\chi^{\,b}$ $(10^{-10}\,\mathrm{s}^{-1})$ | $\zeta_{\mathrm{diss},\ell}/\chi$ $(10^{-11}\,\mathrm{s}^{-1})$ | $\langle p_{\mathrm{diss}} \rangle_\ell$ |
|---|---|---|---|
| (0,0) | 3.08 | 4.13 | 0.134 |
| (0,1) | 3.09 | 4.20 | 0.136 |
| (0,2) | 3.13 | 4.23 | 0.135 |
| (0,3) | 3.15 | 4.57 | 0.145 |
| (0,4) | 3.21 | 4.94 | 0.154 |
| (0,5) | 3.26 | 5.05 | 0.155 |

Photoexcitation and Photodissociation Rates for Unshielded H₂

[Table 31.1, Draine; Draine & Bertoldi (1996)]

Here, the intensity of interstellar radiation field near 1000Å.

$$\chi \equiv \frac{(\nu u_\nu)_{1000\mathring{\mathrm{A}}}}{4 \times 10^{-14}\,\mathrm{erg\,cm}^{-3}}$$

$\chi = 1$ for the ISRF of Habing (1968)
$\quad = 1.71$ for the ISRF of Draine (1978)
$\quad = 1.23$ for the ISRF of Mathis et al. (1983)

▸ In the local diffuse neutral ISM, the H₂ photodissociation rate is:

$$\zeta_{\mathrm{diss}} \equiv \langle p_{\mathrm{diss}} \rangle \, \zeta_{\mathrm{pe}} \approx 5 \times 10^{-11}\,\mathrm{s}^{-1}$$

▸ The typical timescale for photodissociation of H₂ is the: $\quad t_{\mathrm{diss}} \approx 1/\zeta_{\mathrm{diss}} \sim 640\,\mathrm{yr}$

This is smaller by four orders of magnitude that the ~ 15 Myr timescale for creation of H₂ by grain surface catalysis in the CNM.

- Steady-state abundance of $H_2$

▸ The steady-state abundance of molecular hydrogen is determined by a balance between formation on grains and photodissociation, resulting in a very low steady state abundance:

$$\zeta_{\mathrm{diss}} n(\mathrm{H}_2) = R_{\mathrm{gr}} n_{\mathrm{HI}} n_{\mathrm{H}}$$

$$\frac{n(\mathrm{H}_2)}{n_{\mathrm{HI}}} = \frac{R_{\mathrm{gr}} n_{\mathrm{H}}}{\zeta_{\mathrm{diss}}}$$

$$\approx 1.8 \times 10^{-5} \left( \frac{n_{\mathrm{H}}}{30\,\mathrm{cm}^{-3}} \right) \left( \frac{R_{\mathrm{gr}}}{3 \times 10^{-17}\,\mathrm{cm}^3\,\mathrm{s}^{-1}} \right) \left( \frac{5 \times 10^{-11}\,\mathrm{s}^{-1}}{\zeta_{\mathrm{diss}}} \right)$$

▸ *In the absence of self-shielding*, diffuse H I clouds will contain only a tiny amounts of $H_2$. *Molecular hydrogen shouldn't dominate over atomic hydrogen until the density reaches ~ 3x10$^6$ cm$^{-3}$*.

▸ In reality, observations reveal that the molecular form dominates at densities as low as ~ 300 cm$^{-3}$. This is because the inner parts of molecular clouds are protected from UV light by *self-shielding*.

# Self-Shielding and Dust-Shielding

- *Self-shielding* refers to the phenomenon where the photoexcitation transitions become optically thick, so that the molecule in question is "shielded" from starlight by other molecules.

  ‣ Self-shielding occurs on a line-by-line basis, with stronger self-shielding for the stronger lines (large oscillator strengths) from levels with large populations.

  ‣ Recall that the equivalent width is the measure of absorbed light (EW = fraction of absorbed light). **The rate of photoexcitation** is given, in general, by

$$\Delta N_\ell \zeta_{\mathrm{pe},\ell\to u} = \left(\frac{u_\nu c}{h\nu}\right)\Delta W$$

$$\zeta_{\mathrm{pe},\ell\to u} = \left(\frac{u_\nu c}{h\nu}\right)_{\ell u}\frac{dW_\nu}{dN_\ell}$$

where

$$W_\nu = \int d\nu\left(1 - e^{-\tau_\nu}\right)$$

$$\tau_\nu = N_\ell \chi_0 \phi_\nu = N_\ell \frac{\pi e^2}{m_e c}f_{\ell u}\phi_\nu$$

$$\phi_\nu = \text{line profile}$$

$u_\nu$ = radiation energy density in the absence of H$_2$ line absorption

In the optical thin limt,

$$\frac{dW_\nu}{dN_\ell} = \frac{d}{dN_\ell}\int d\nu\,\tau_\nu = \chi_0 = \frac{\pi e^2}{m_e c}f_{\ell u}$$

Note that
$$\tau_\lambda = \tau_\nu = N_\ell \frac{\pi e^2}{m_e c}f_{\ell u}\phi_\lambda\left|\frac{d\lambda}{d\nu}\right|$$

  ‣ Therefore, the self-shielding factor is defined to be:

$$f_{\mathrm{shield},\ell u} \equiv \frac{dW_\nu/dN_\ell}{(\pi e^2/m_e c)f_{\ell u}} < 1 \quad\longrightarrow\quad \zeta_{\mathrm{pe},\ell\to u} = \left(\frac{u_\nu c}{h\nu}\right)_{\ell u}\left(\frac{\pi e^2}{m_e c}f_{\ell u}\right)f_{\mathrm{shield},\ell u}$$

▸ The photodissociation rate for H₂ in level $\ell$ is reduced by self-shielding:

$$\zeta_{\text{diss},\ell} = \sum_u \zeta_{\text{pe},\ell \to u} p_{\text{diss},u}$$

$$= \frac{\pi e^2}{m_e c} \sum_u f_{\ell u} \left( \frac{u_\nu c}{h\nu} \right)_{\ell u} f_{\text{shield},\ell u} p_{\text{diss},u}$$

> Compare with Eq. (31.24) of [Draine]
>
> $$u_\nu = u_\lambda \left| \frac{d\lambda}{d\nu} \right| = u_\lambda \frac{\lambda^2}{c}$$
>
> $$\rightarrow \frac{u_\nu c}{h\nu} = u_\lambda \frac{\lambda^3}{hc}$$

▸ The photodissociation rate per H₂ is obtained by averaging the above equation over the population levels. A reasonably accurate approximation is given by Draine & Bertoldi (1996).

$$\zeta_{\text{diss}} \approx \zeta_{\text{diss},0} f_{\text{shield, diss}} e^{-\tau_{\text{d},1000}}$$

$$f_{\text{shield,diss}} \approx \frac{0.95}{(1 + x/b_5)^2} + \frac{0.035}{(1 + x)^{0.5}} \exp\left[-8.5 \times 10^{-4}(1 + x)^{0.5}\right]$$

$$x \equiv \frac{N(\text{H}_2)}{5 \times 10^{14} \text{ cm}^{-2}}, \quad b_5 \equiv \frac{b}{\text{km s}^{-1}}$$

$\zeta_{\text{diss},0}$  = the photodissociation rate in the absence of dust extinction or self-shielding

$\tau_{\text{d},1000}$  = the dust optical depth by dust at 1000Å.

- ▸ Ryden provides a crude approximation for the self-shielding factor:

$$f_{\text{shield,diss}} \approx \left( \frac{N(\text{H}_2)}{10^{14} \, \text{cm}^{-2}} \right)^{-3/4}$$

- ▸ For a cloud with a density of 1000 cm$^{-3}$,

$$\frac{n(\text{H}_2)}{n_{\text{HI}}} = \frac{R_{\text{gr}} n_{\text{H}}}{\zeta_{\text{diss}}}$$

> $n_{\text{H}}$ = number density of H nucleon
> $n_{\text{HI}}$ = number density of H atom

$$\approx 6 \times 10^{-4} \left( \frac{n_{\text{H}}}{1000 \, \text{cm}^{-3}} \right) \left( \frac{1}{f_{\text{shield,diss}}} \right)$$

The ratio of H$_2$ molecules to H atoms becomes equal to one when the gas is self-shielded by a column density:

$$N_{\text{H}_2} \gtrsim 1.5 \times 10^{18} \, \text{cm}^{-2} \qquad \leftarrow \frac{n(\text{H}_2)}{n_{\text{HI}}} = 1$$

This corresponds to **an outer shelf-shielding skin to the cloud that is just 4x10$^{-4}$ pc.**

$$d = \frac{N_{\text{H}_2}}{n_{\text{H}}} = 4 \times 10^{-4} \, \text{pc} \left( \frac{N_{\text{H}_2}/1.5 \times 10^{18} \, \text{cm}^{-2}}{n_{\text{H}}/1000 \, \text{cm}^{-3}} \right)$$
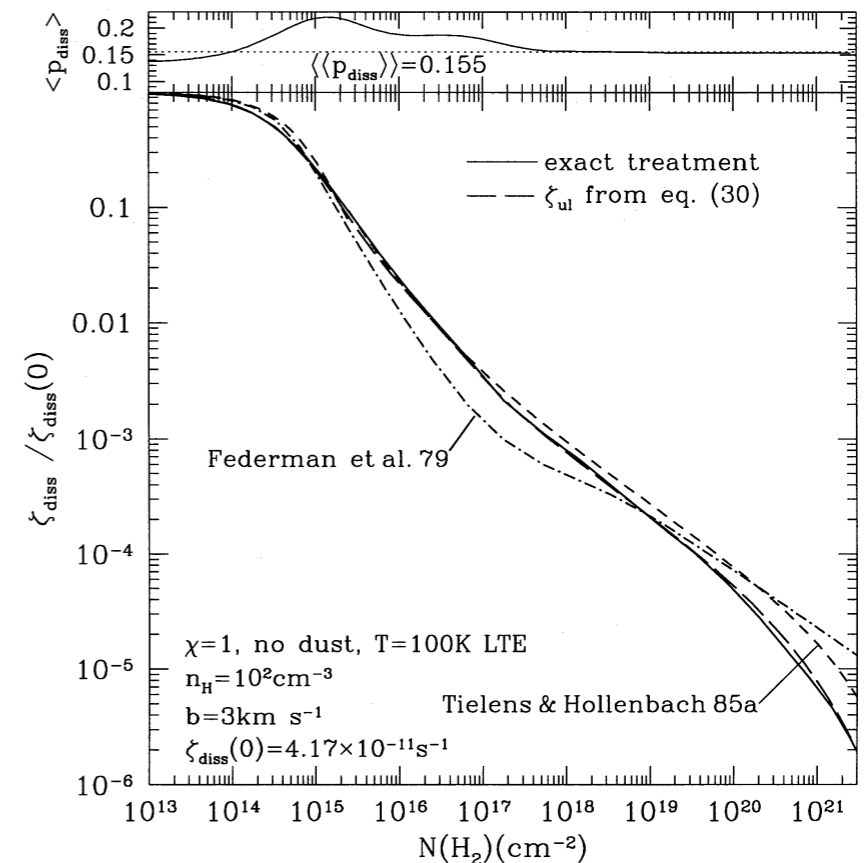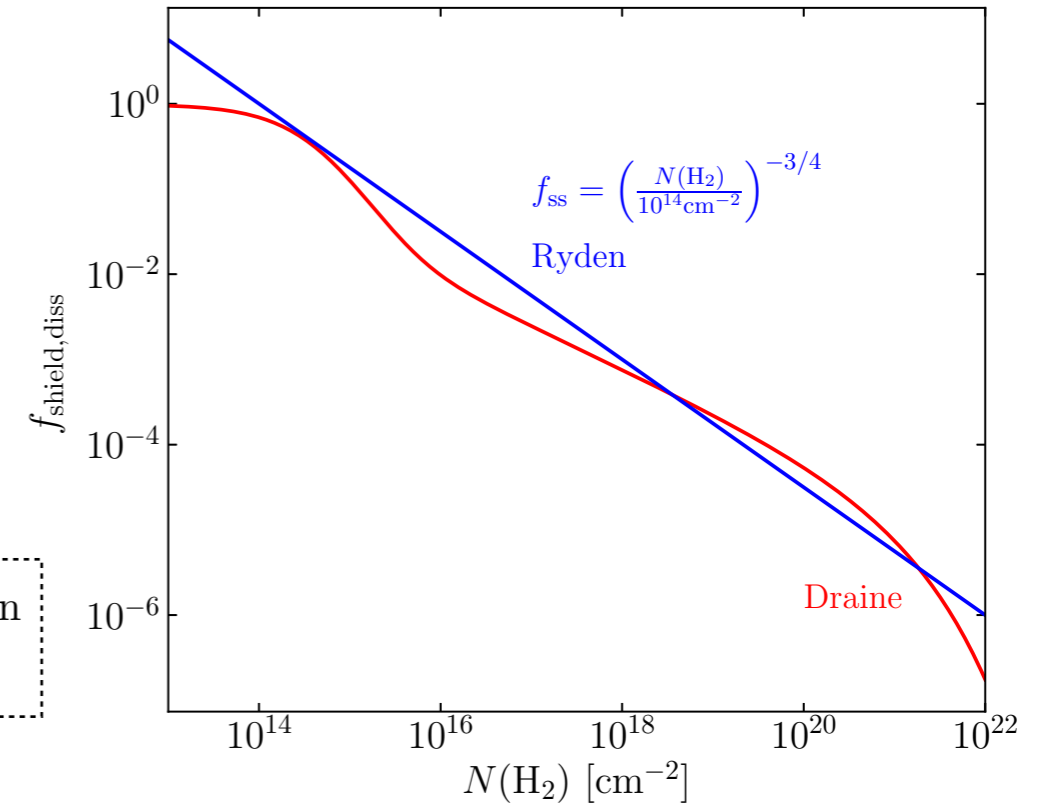


Fig 1, Draine & Bertoldi (1996)

- **Dust** can also shield molecular gas from UV light.

  ‣ In our galaxy, the relation between dust extinction and column density of hydrogen nucleon and the ratio between extinctions 1100Å and V band are, respectively:

  $$\frac{A_V}{N_{\mathrm{H}}} \approx 5.3 \times 10^{-22} \ \mathrm{cm}^2 \qquad\qquad \frac{A_{1100}}{A_V} \approx 4$$

  ‣ When hydrogen is primarily molecular, $N(\mathrm{H}_2) = N_{\mathrm{H}}/2$. This results in dust extinction in the Lyman and Werner bands of

  $$\frac{A_{1100}}{N(\mathrm{H}_2)} \approx \frac{4A_V}{N_{\mathrm{H}}/2} \approx 4.2 \times 10^{-21} \ \mathrm{cm}^2$$

  ‣ Thus, column densities $N(\mathrm{H}_2) \gtrsim 2.4 \times 10^{20} \ \mathrm{cm}^{-2}$ have more than one magnitude of dust extinction in the Lyman and Werner bands. $A_{1100} \gtrsim 1$

  ‣ This is 100 times higher than the $H_2$ column density that leads to self-shielding in typical molecular gas. Thus, **self-shielding by $H_2$ is much more effective than shielding by dust under ordinary circumstances.**

# Vibrational and Rotational Level Population

- Vibrational Level Populations

  - Photoexcitation to some level $B(v', J')$ or $C(v', J')$ will be followed, within a few nanoseconds, by spontaneous decay to some level $X(v'', J'')$ of the ground electronic state. As a result, UV pumping of H₂ populates the vibrationally excited levels of the ground electronic state.

  - At low densities, these vibrationally excited levels will spontaneously decay to lower vibrational levels via electric quadrupole transitions. *This "radiative cascade" populates many lower levels, finally reaching the ground vibrational level.*

  - The vibrationally excited levels have radiative lifetimes of only ~ 10⁶ sec, and collisional deexcitation by collisions with H, H₂, or He is unlikely at densities $n_{\rm H} \lesssim 10^4 \, {\rm cm}^{-3}$.

- Rotational Level Populations

  - In the ground vibrational state, the lifetime of the lowest rotational levels are long enough that collisional effects can play a role in depopulating the lowest J levels. **_The populations of the lowest J levels are, therefore, sensitive to the density and temperature of the gas._**

  - For **_low levels of self-shielding_** ($N(\mathrm{H_2}) \lesssim 10^{15}\,\mathrm{cm}^{-2}$), the rotational distribution function for J > 2 is relatively insensitive to the gas temperature.

    ‣ The rotational levels $J \geq 3$ have relative populations that can be approximately characterized by rotational temperature $T_{\mathrm{rot}} \approx 400\,\mathrm{K}$.

    ‣ However, this has nothing to do with the actual temperature; **_it is entirely the result of the branching ratios in the vibration-rotation "cascade" that populates the high J levels_**.

  - **_As the shielding column density increases_**, the UV pumping rates decline, and the fraction of $H_2$ in levels J > 3 declines.

    ‣ The relative populations of levels J = 0 and J = 2 can be used to estimate the gas temperature:
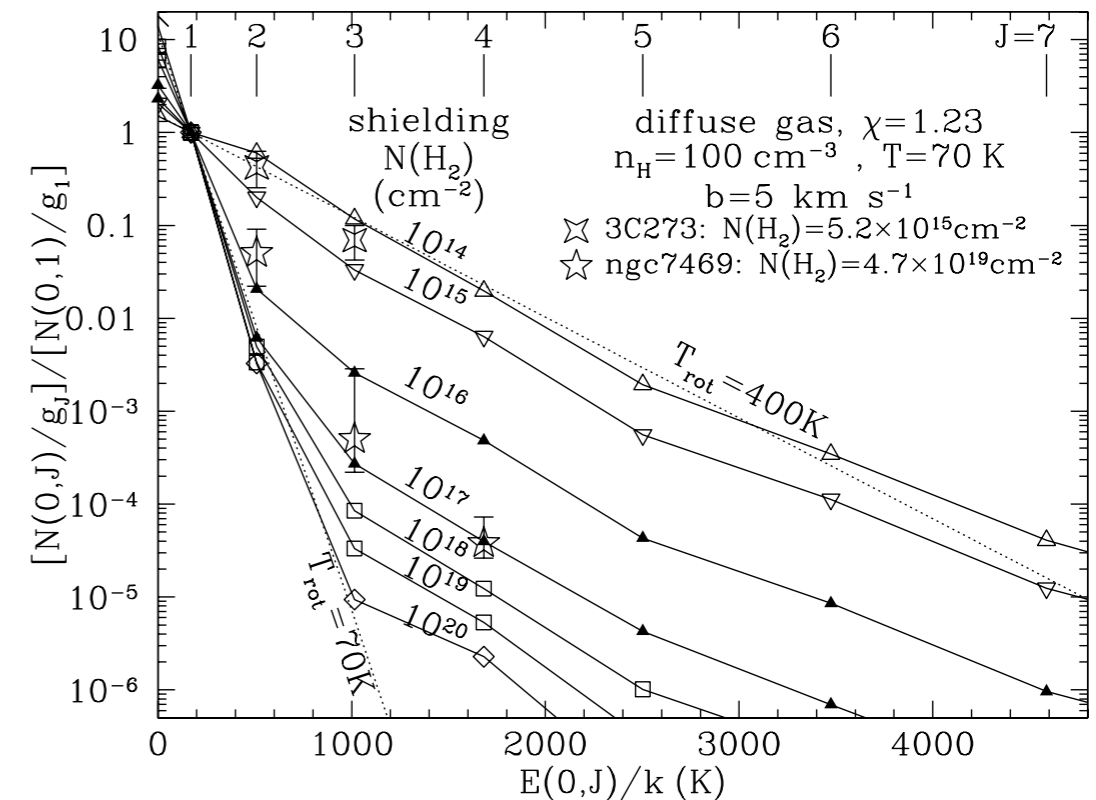


Rotational excitation of $H_2$ in diffuse clouds, for various $N(\mathrm{H_2})$.

Also shown is the rotational excitation of $H_2$ in diffuse clouds to the sightlines of the AGNs 3C273 and NGC 7469 (Gillmon et al. 2006).
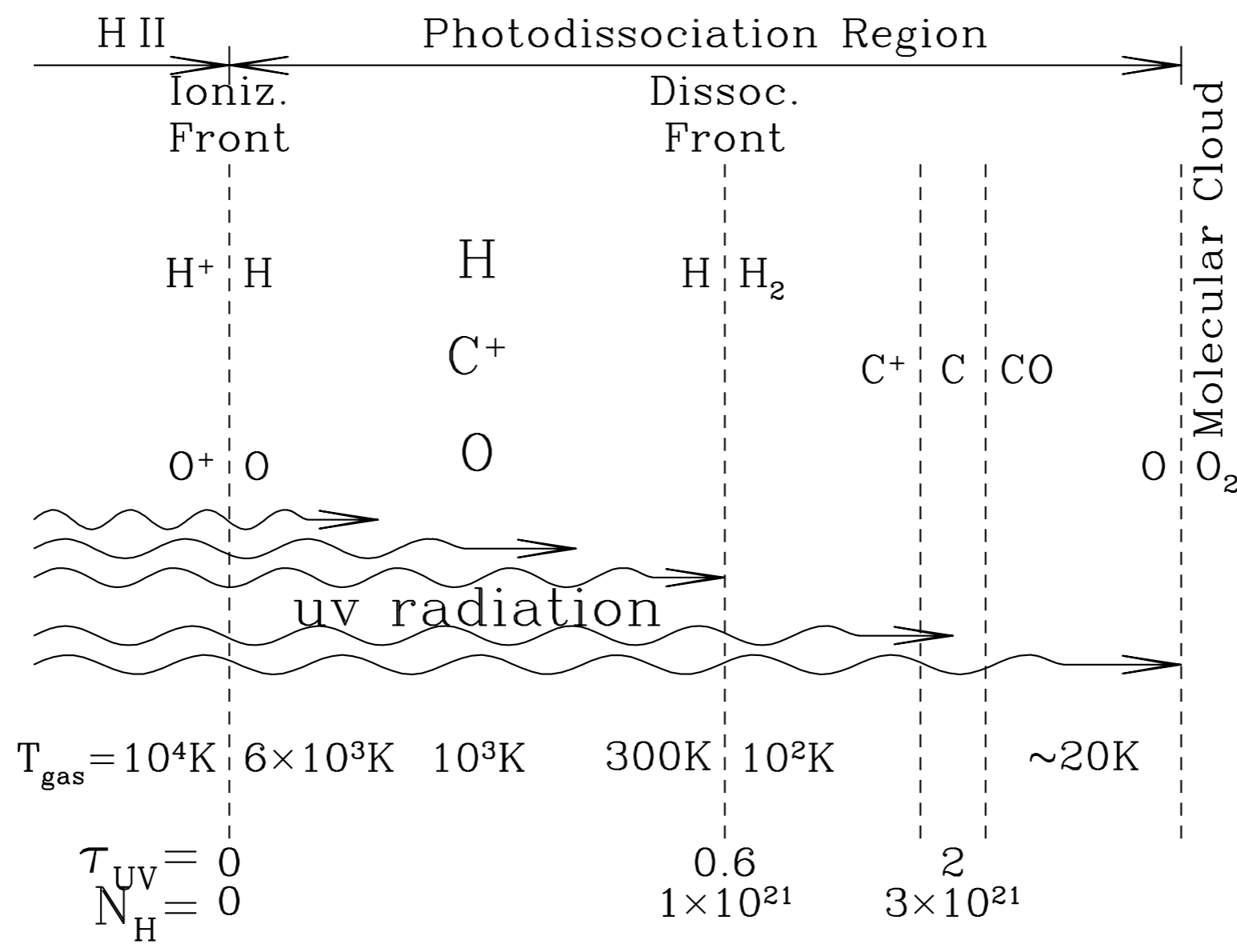
Fig 31.1, Draine

For $N(\mathrm{H_2}) \gtrsim 10^{18}\,\mathrm{cm}^{-2}$  high column density

$$T_{\mathrm{gas}} \approx \frac{510\,\mathrm{K}}{\ln\left[5N(0,0)/N(0,2)\right]}$$

# Photodissociation Region (PDR)

- H II region + PDR

  - Stars are formed out of molecular gas, and when a massive star forms, it strongly irradiate the remaining molecular clouds with UV radiation, resulting in photoionization and photodissociation.

    ‣ The photoionized gas, heated to $\sim 10^4$ K, will be overpressure, which will drive a compressive wave in the molecular cloud, and will also cause the ionized gas to try to flow toward lower-pressure regions nearby.

    ‣ **The interface between the H II region and the dense molecular cloud is called a photodissociation region or PDR.**

    ‣ PDR will be bounded by an ionization front - the surface where the hydrogen is 50% ionized - and will contain a photodissociation front - the surface where the hydrogen is 50% atomic and 50% molecular (by mass).

  - The overall physics and chemistry of PDRs is complex - see the review by Hollenbach & Tielens (1999).

H II

Photodissociation Region

Ioniz.
Front

Dissoc.
Front

Molecular Cloud

$H^+$ ⁞ H

H

H ⁞ $H_2$

$C^+$

$C^+$ ⁞ C ⁞ CO

$O^+$ ⁞ O

O

O ⁞ $O_2$

uv radiation

$T_{gas} = 10^4K$ ⁞ $6\times10^3K$   $10^3K$   $300K$ ⁞ $10^2K$     $\sim20K$

$\tau_{UV} = 0$                                     0.6          2
$N_H = 0$                                     $1\times10^{21}$     $3\times10^{21}$

Structure of a PDR at the interface between an H II region
and a dense molecular cloud.

[Fig 31.2, Draine]

# [Molecular Clouds] Observations

- Cloud Structure

    - Local density estimates using line ratios often give larger densities than global mean densities found by averaging the observed molecular column densities along the line of sight.

    - The interpretation of this is that the ***clouds are very clumpy***, with the dense cores having typical sizes of < 1 pc or smaller, and densities > $10^6$ cm$^{-3}$.

    - The overall cloud extends for 3—20 pc on average, with a mean density of $10^{3-4}$ cm$^{-3}$.

    - Most molecular clouds show **a number of discernible cores**. These are often detected as sources of molecular lines with high critical densities (e.g., CS), while the general cloud is mapped using lines of lower critical density (mainly CO).

    - Within the galaxies, molecular clouds are most often seen organized into complexes with **sizes from 20 pc to 100 pc, and overall H$_2$ masses of $10^{4-6}$ $M_{sun}$**. The distinction between "clouds" and "complexes" in terms of sizes and masses is somewhat artificial. A more precise statement would be that ***we see a wide range of structures***, from single small clouds to large complexes of clouds, with many complexes arrayed along the spiral arms of the Galaxy.

# Molecular Clouds: Cloud Categories

- Cloud Categories (based on the total surface density)

  - Individual clouds are separated into categories based on their optical appearance: diffuse, translucent, or dark, depending on the visual extinction $A_V$ through the cloud.

| Category | $A_V$ (mag) | Examples |
|---|---|---|
| Diffuse Molecular Cloud | $\lesssim 1$ | $\zeta$ Oph cloud, $A_V = 0.84$ [a] |
| Translucent Cloud | 1 to 5 | HD 24534 cloud, $A_V = 1.56$ [b] |
| Dark Cloud | 5 to 20 | B68 [c], B335 [d] |
| Infrared Dark Cloud (IRDC) | 20 to $\gtrsim 100$ | IRDC G028.53-00.25 [e] |

[a] van Dishoeck & Black (1986).
[b] Rachford et al. (2002).
[c] Lai et al. (2003).
[d] Doty et al. (2010).
[e] Rathborne et al. (2010).

[Table 32.1, Draine]

  - **Diffuse and translucent clouds** have sufficient UV radiation to keep gas-phase carbon mainly photoionized throughout the cloud.

    ‣ Such clouds are usually pressure-confined, although self-gravity may be significant in some cases.

  - The typical **dark clouds have $A_V \sim$ 10 mag, and is self-gravitating**. Some dark clouds contain dense regions that are extremely opaque, with $A_V > 20$ mag.

  - **Infrared Dark Clouds** are opaque even at 8 μm, and can be seen in silhouette against a background of diffuse 8 μm emission from PAHs in the ISM.

- Terminology for Cloud Complexes and Their Components

| Categories | Size (pc) | $n_{\mathrm{H}}$ ($\mathrm{cm}^{-3}$) | Mass ($M_\odot$) | Linewidth ($\mathrm{km\,s}^{-1}$) | $A_V$ (mag) | Examples |
|---|---|---|---|---|---|---|
| GMC Complex | $25-200$ | $50-300$ | $10^5-10^{6.8}$ | $4-17$ | $3-10$ | M17, W3, W51 |
| Dark Cloud Complex | $4-25$ | $10^2-10^3$ | $10^3-10^{4.5}$ | $1.5-5$ | $4-12$ | Taurus, Sco-Oph |
| GMC | $2-20$ | $10^3-10^4$ | $10^3-10^{5.3}$ | $2-9$ | $9-25$ | Orion A, Orion B |
| Dark Cloud | $0.3-6$ | $10^2-10^4$ | $5-500$ | $0.4-2$ | $3-15$ | B5, B227 |
| Star-forming Clump | $0.2-2$ | $10^4-10^5$ | $10-10^3$ | $0.5-3$ | $4-90$ | OMC-1, 2, 3, 4 |
| Core | $0.02-0.4$ | $10^4-10^6$ | $0.3-10^2$ | $0.3-2$ | $30-200$ | B335, L1535 |

[Table 32.2, Draine]

- The **giant molecular cloud (GMC)** and **dark cloud** categories are distinguished mainly by total mass.

- Groups of distinct clouds are referred to as **cloud complexes**.

  ▸ Molecular clouds are sometimes found in isolation, but in many cases molecular clouds are grouped together into complexes.

  ▸ Since large clouds generally have substructure, the distinction between "cloud" and "cloud complex" is somewhat arbitrary.

  ▸ Delineation of structure in cloud complexes is guided by the intensities and radial velocities of molecular lines (e.g., CO J = 1-0) as well as maps of thermal emission from dust at submm wavelengths.

| Categories | Size (pc) | $n_{\mathrm{H}}$ ($\mathrm{cm}^{-3}$) | Mass ($M_\odot$) | Linewidth ($\mathrm{km\,s}^{-1}$) | $A_V$ (mag) | Examples |
|---|---|---|---|---|---|---|
| GMC Complex | $25-200$ | $50-300$ | $10^5-10^{6.8}$ | $4-17$ | $3-10$ | M17, W3, W51 |
| Dark Cloud Complex | $4-25$ | $10^2-10^3$ | $10^3-10^{4.5}$ | $1.5-5$ | $4-12$ | Taurus, Sco-Oph |
| GMC | $2-20$ | $10^3-10^4$ | $10^3-10^{5.3}$ | $2-9$ | $9-25$ | Orion A, Orion B |
| Dark Cloud | $0.3-6$ | $10^2-10^4$ | $5-500$ | $0.4-2$ | $3-15$ | B5, B227 |
| Star-forming Clump | $0.2-2$ | $10^4-10^5$ | $10-10^3$ | $0.5-3$ | $4-90$ | OMC-1, 2, 3, 4 |
| Core | $0.02-0.4$ | $10^4-10^6$ | $0.3-10^2$ | $0.3-2$ | $30-200$ | B335, L1535 |

[Table 32.2, Draine]

- Structures within a cloud (self-gravitating entities) are described as **clumps**.

  ‣ Clumps may or may not be forming stars; in the former case they are termed **star-forming clumps**. **Cores** are density peaks within star-forming clumps that will form a single star or a binary star.

- GMC and GMC complex

  ‣ Much of the molecular mass is found in large clouds known as "giant molecular clouds", with masses ranging from $\sim 10^3\,M_\odot$ to $\sim 2.5 \times 10^5\,M_\odot$. Theses have reasonably well-defined boundaries.

  ‣ A GMC complex is a gravitationally bound group of GMCs (and smaller clouds) with a total mass $\gtrsim 10^{5.3}\,M_\odot$.
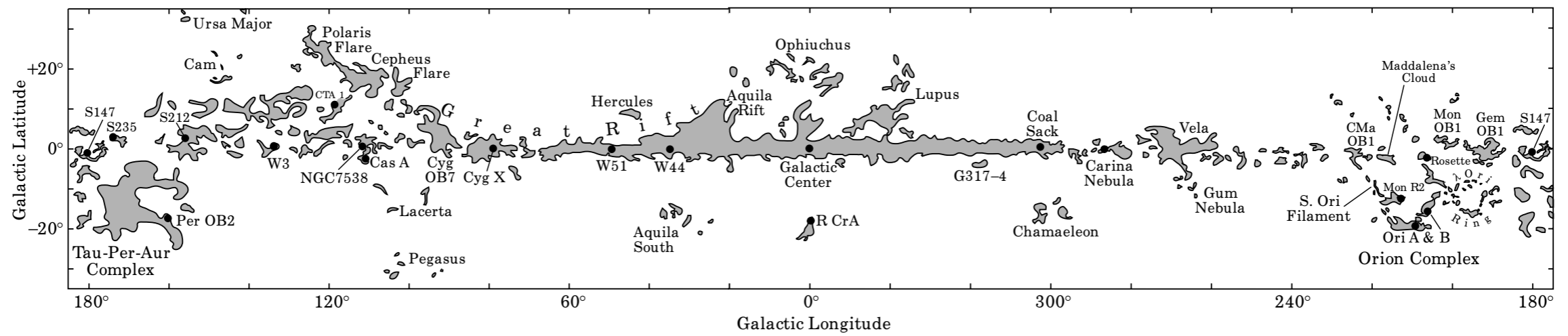
Locations of prominent molecular clouds along the Milky Way

[Fig 32.2, Draine, Dame et al. (2001)]

# Mass Distribution of GMCs

- Overall mass distribution of GMCs in the Milky Way

  - CO line surveys can detect GMCs at large distances, allowing the total number in the Galaxy to be estimated.

  - The overall mass distribution of GMCs in the Milky Way (excluding the molecular material within a few hundred pc of the Galactic center) can be approximated by a power-law:

$$\frac{dN_{\mathrm{GMC}}}{d\ln M_{\mathrm{GMC}}} \approx N_u \left( \frac{M_{\mathrm{GMC}}}{M_u} \right)^{-\alpha} \quad \text{for} \quad 10^3\, M_\odot \lesssim M_{\mathrm{GMC}} < M_u$$

$$M_u \approx 6 \times 10^6 M_\odot$$
$$N_u \approx 63$$
$$\alpha \approx 0.6$$

  - Most of the mass is in the most massive GMCs:

    ▸ ~ 80% of the molecular mass is in GMCs with $M > 10^5\, M_\odot$.

- **Star Counts**
  - Molecular clouds were originally discovered by star counts.
    - ▸ Herschel (1785) noticed that there were patches along the Milky Way where very few stars were seen. He incorrectly attributed this to a real absence of stars.
    - ▸ We now understand that the apparent deficiency of stars is the result of obscuration by dusty clouds.
    - ▸ Star counts using background stars is a good way to study the cloud structure.
    - ▸ Because the visual obscuration can be very large, studies of dark clouds using star counts are now usually done in the J, H, or K bands.

# Gas Surface Density in the Milky Way

- The most common way to study molecular gas is through molecular line emission, and the primary line used is the J = 1-0 transition (2.6 mm) of CO.

  ‣ This transition is often optically thick, but the CO 1-0 luminosity of a cloud is approximately proportional to the total mass.

  ‣ *Velocity-resolved mapping of CO 1-0 together with an assumed rotation curve and an adopted value of the "CO to H₂ conversion factor" X_CO have been used to infer the surface density of H₂ over the Milky Way disk.*

Gas surface densities as a function of galactocentric radius. The Sun is assumed to be at R = 8.5 kpc.

- Surface density of H₂ estimated from CO 1-0 observations (Nakanishi & Sofue 2006), assuming

$$X_{\mathrm{CO}} = 1.8 \times 10^{20}\,\mathrm{H_2\,cm^{-2}/K\,km\,s^{-1}}$$

- Surface density of H II derived from pulsar dispersion measures (Cordes & Lazio 2003).
- Surface density of H I from 21-cm studies (Nakanishi & Sofue 2003)

[Fig 32.4, Draine]



$M(\mathrm{HII+HI+H_2+He}) = 6.7 \times 10^9\,M_\odot$

$M(\mathrm{HI}) = 2.9 \times 10^9\,M_\odot$
$M(\mathrm{HII}) = 1.1 \times 10^9\,M_\odot$
$M(\mathrm{H_2}) = 8.4 \times 10^8\,M_\odot$

$5.\exp[-(R-12\mathrm{kpc})/3.5\mathrm{kpc}]$
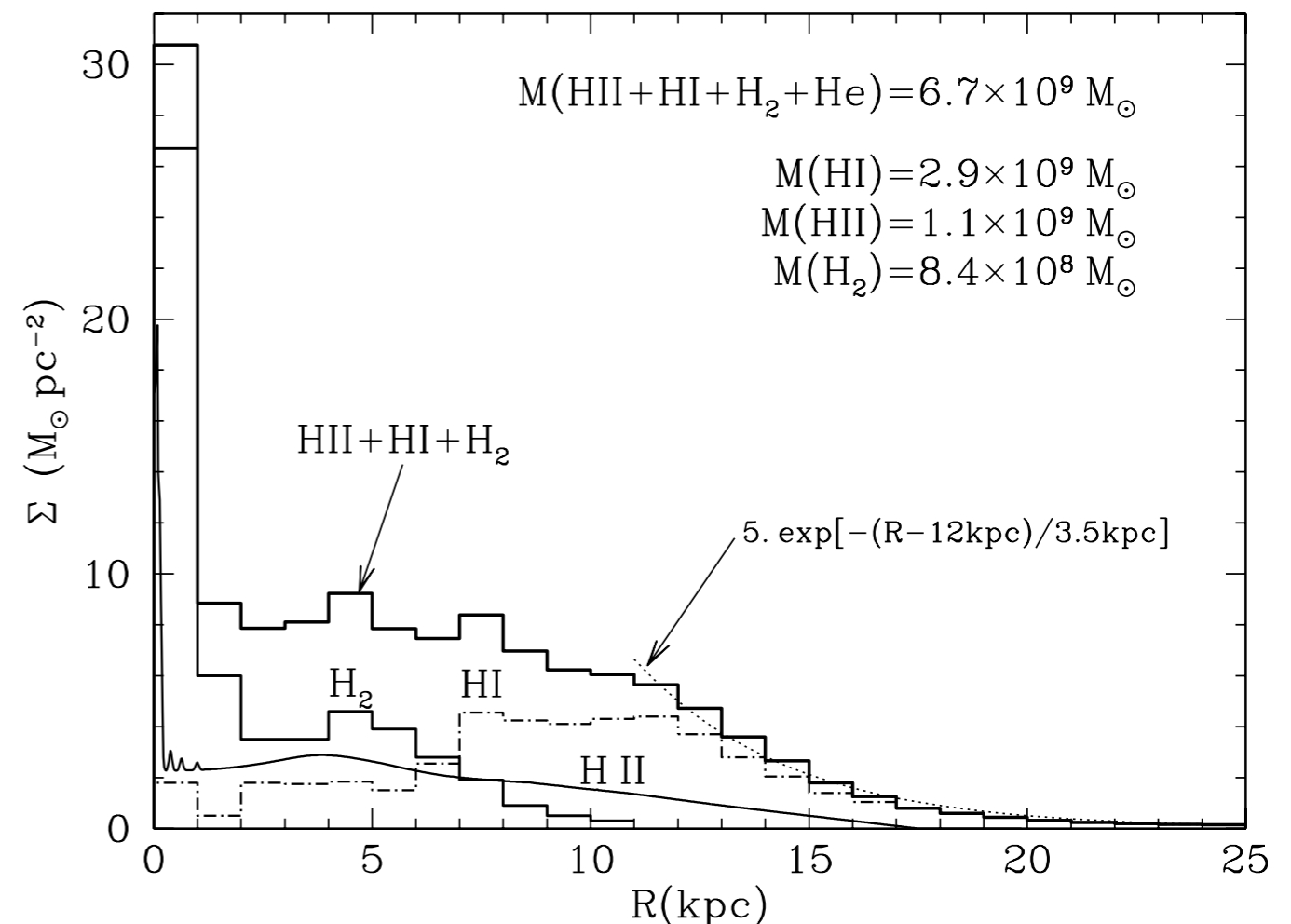
# Size-Linewidth Relation in Molecular Clouds

- Larson (1981) noted that observations of molecular clouds in spectral lines of CO, $H_2CO$, $NH_3$, OH, and other species, were broadly consistent with a ***size-linewidth relation***, where a density peak of characteristic size $L$ tends to have a <u>3D velocity dispersion</u> given by

$$\sigma_v^* \approx 1.10\, L_{\mathrm{pc}}^{\gamma}\, \mathrm{km\, s}^{-1}, \quad \gamma \approx 0.38 \ \text{ for } 0.01 \lesssim L_{\mathrm{pc}} \lesssim 10^2 \ \ (L_{\mathrm{pc}} = L/\mathrm{pc})$$

where $L$ is the maximum projected dimension of the density peak.

▸ Larson noted that the power-law index $\gamma \approx 0.38$ is curiously close to the index 1/3 found by **Kolmogorov** for a turbulent cascade in an incompressible fluid.

▸ It therefore is tempting to refer to the observed fluid motion as "turbulence," although in realty the motions are some combination of thermal motions, rotation, MHD waves, and turbulence.

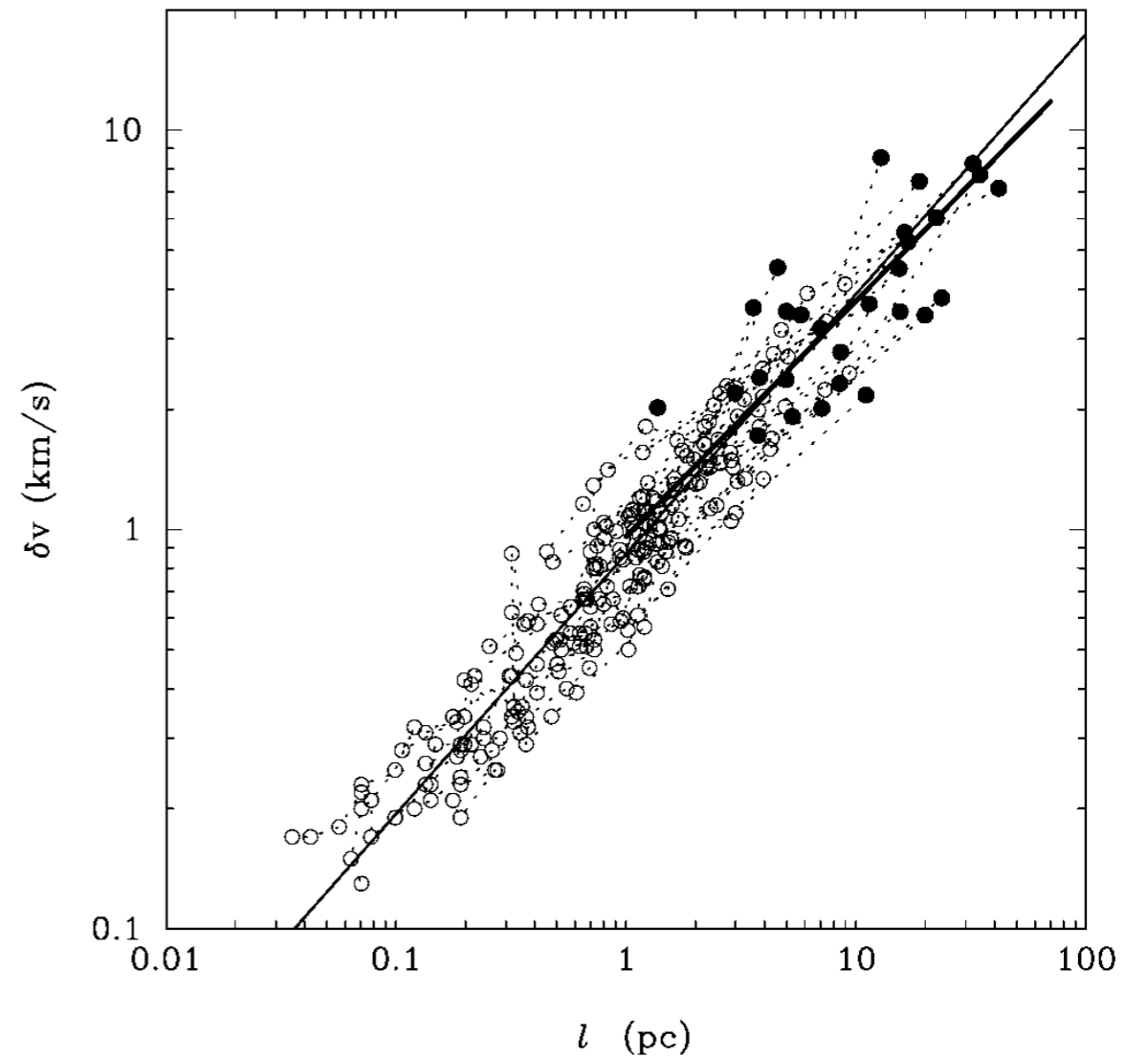The 3D internal velocity dispersion versus maximum linear dimension $L$ of the density peak.

Fig 32.5, Draine; Larson (1981)
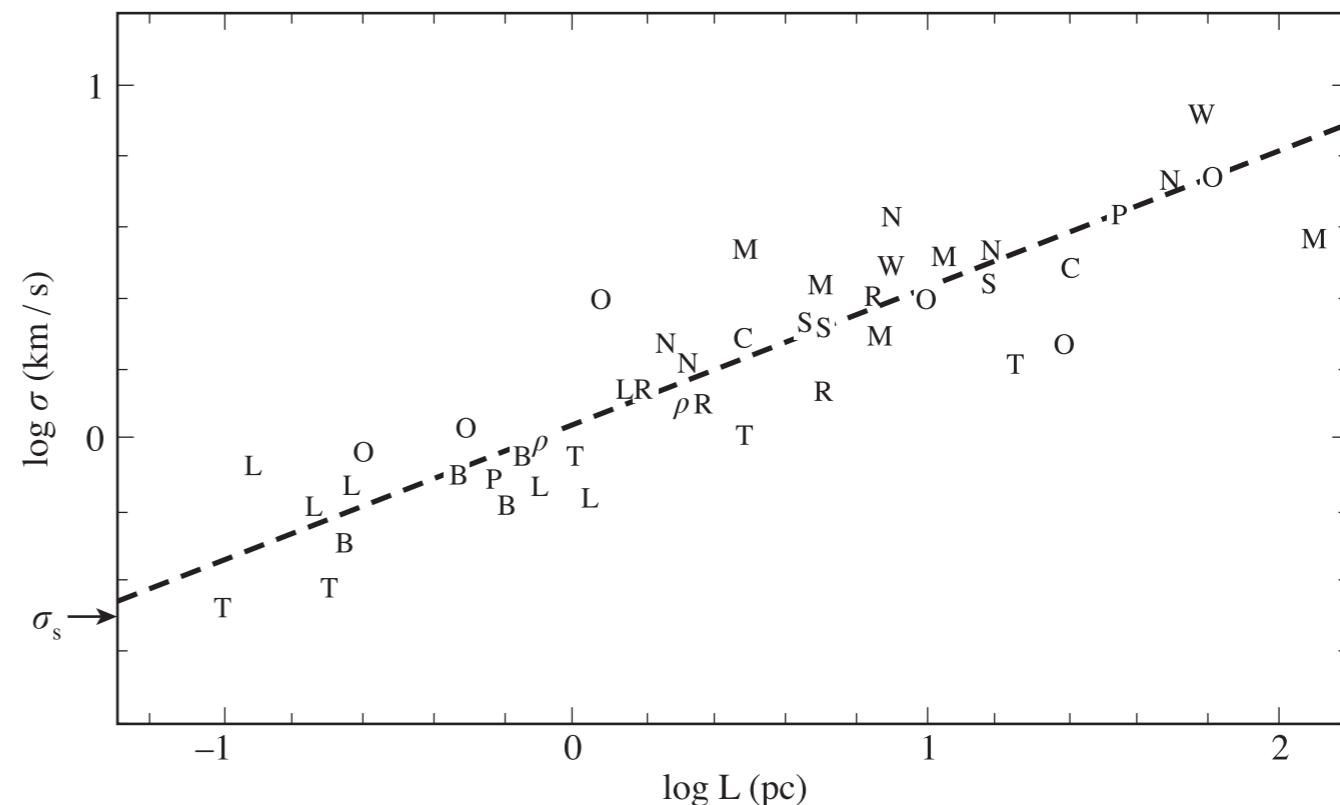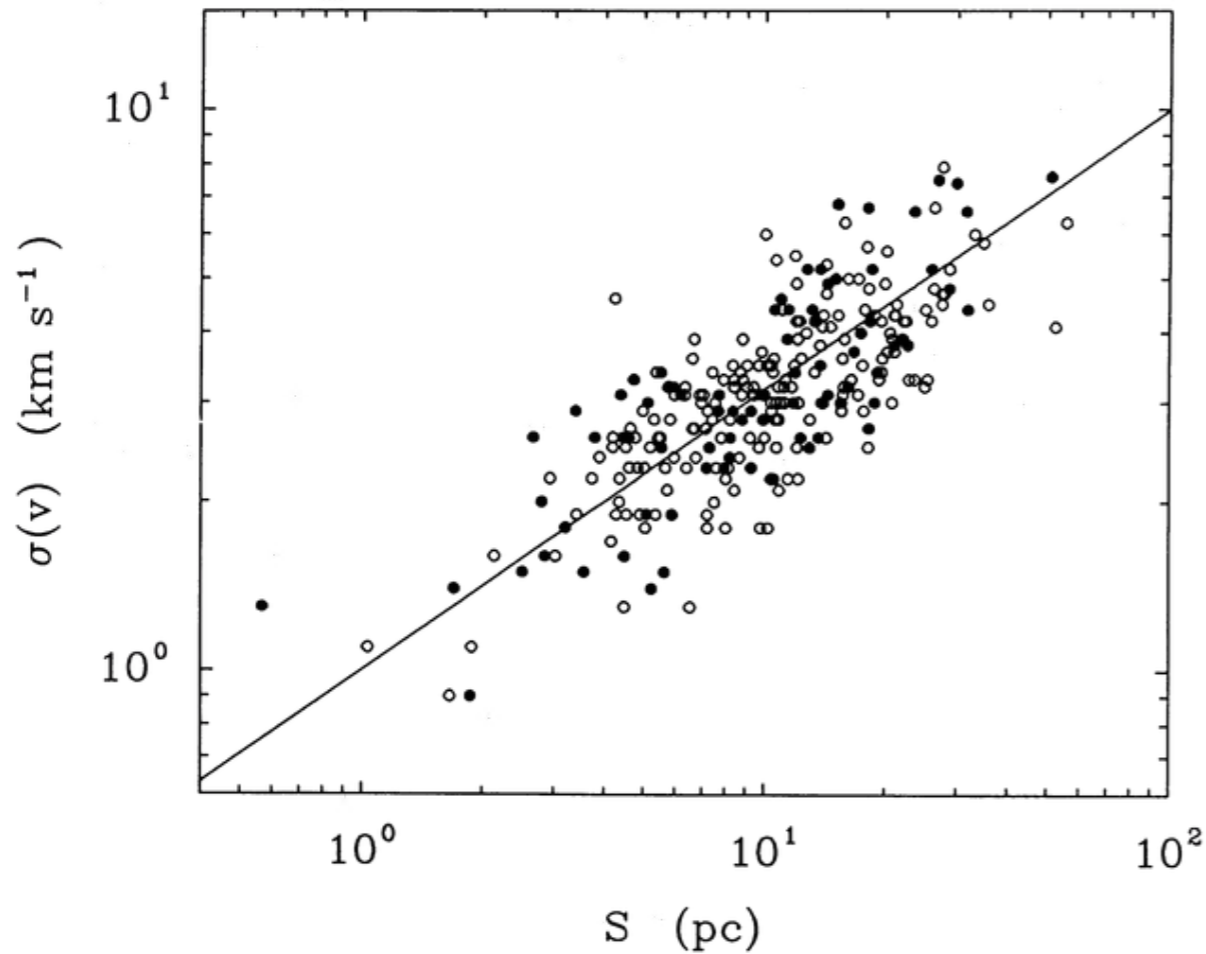
Molecular cloud velocity dispersion as a function of size $S$ for 273 clouds in the Galaxy

Fig 1, Solomon et al. (1987)

Velocity dispersion versus size $\ell$ from PCA decomposition of $^{12}CO$ J = 1-0 imaging observations of 27 individual molecular clouds

Fig 1, Heyer & Brunt (2004)

- However, the power-law index $\gamma \approx 0.38$ has been questioned.

  ▸ Solomon et al. (1987) found $\sigma_v^* \approx 1.0\, L_{\mathrm{pc}}^{0.5}\, \mathrm{km\, s^{-1}}$ from a study of 273 molecular clouds.

  ▸ Heyer & Brunt (2004) found $\sigma_v^* \approx 0.96\, L_{\mathrm{pc}}^{0.59}\, \mathrm{km\, s^{-1}}$.

- Note that

  ▸ For $L \gtrsim 0.02\, \mathrm{pc}$, $\sigma_v^* \gtrsim (kT/\mu)^{1/2} \approx 0.23(T/15\, \mathrm{K})^{1/2}\, \mathrm{km\, s^{-1}}$ ⇒ The linewidth is supersonic.

  ▸ For $L \lesssim 0.02\, \mathrm{pc}$, the line width is nearly thermal, with only a small contribution from rotation, waves or turbulence.

- The density peaks are generally self-gravitating. If we assume them to be in approximate virial equilibrium, and consider only the kinetic energy associated with fluid motions, we can estimate the clump mass using the virial theorem.

  ▸ For a uniform density sphere with a diameter $L$, we can obtain the follows:

$$\sigma_v^{*2} = 3\sigma_v^2 = 6GM/5L \quad (L = 2R)$$

> However, this gives $\sigma_v^* \propto L$, which is not consistent with the size-linewidth relation

for $\gamma \approx 0.38$

| | | |
|---|---|---|
| clump mass: | $M \approx \dfrac{5\sigma_v^{*2}L}{6G} \approx 230\, L_{\mathrm{pc}}^{2\gamma+1}\, M_\odot$ | $\rightarrow\quad 230\, L_{\mathrm{pc}}^{1.76}\, M_\odot$ |
| density: | $n_{\mathrm{H}} \approx M/[(4\pi/3)(L/2)^3 1.4m_{\mathrm{H}}] \approx 1.3 \times 10^4\, L_{\mathrm{pc}}^{2\gamma-2}\, \mathrm{cm^{-3}}$ | $\rightarrow\quad 1.3 \times 10^4\, L_{\mathrm{pc}}^{-1.24}\, \mathrm{cm^{-3}}$ |
| column density: | $N_{\mathrm{H}} = n_{\mathrm{H}}L \approx 4.0 \times 10^{22}\, L_{\mathrm{pc}}^{2\gamma-1}\, \mathrm{cm^{-2}}$ | $\rightarrow\quad 4.0 \times 10^{22}\, L_{\mathrm{pc}}^{-0.24}\, \mathrm{cm^{-2}}$ |

▸ We recall that for the dust in diffuse clouds, $A_V/N_{\rm H} = 1.87 \times 10^{21}\,{\rm cm}^2$ , and we would have

$$A_V \approx 21\,L_{\rm pc}^{2\gamma-1}\,{\rm mag} \quad \rightarrow \quad 21\,L_{\rm pc}^{-0.24}\,{\rm mag}$$

The dust in dense clouds differs from that in the diffuse ISM, but this would give a reasonable estimate of the visual extinction through the cloud.

▸ If $\gamma \approx 0.38$, then **a GMC complex** with diameter $L \approx 50\,{\rm pc}$ would have

$$M \approx 2 \times 10^5\,M_\odot$$
$$n_{\rm H} \approx 100\,{\rm cm}^{-3}$$
$$A_V \approx 8\,{\rm mag}$$

whereas **a core** with diameter $L \approx 0.1\,{\rm pc}$ would have

$$M \approx 4\,M_\odot$$
$$n_{\rm H} \approx 2 \times 10^5\,{\rm cm}^{-3}$$
$$A_V \approx 40\,{\rm mag}$$

- Comments on the exponent: $N_{\mathrm{H}} \approx 4.0 \times 10^{22} L_{\mathrm{pc}}^{2\gamma-1}$

  ‣ If $\gamma < 0.5$, smaller clouds tend to have a higher column density, meaning to be darker.

  ‣ If $\gamma = 0.5$, small clouds and large clouds would all have the same column density and dust extinction ($A_V$).

  ‣ However, **observationally, smaller structures tend to have higher $A_V$. This is consistent with exponent $\gamma < 0.5$.**

  ‣ Therefore, *the Larson's exponent would be better constrained with the observations*.

- Expressing the above relations with density as the independent variables, we obtain

$$L_{\mathrm{pc}} = (n_3/13)^{1/(2\gamma-2)} \qquad \rightarrow 7.94\, n_3^{-0.81} \quad ,$$

$$\sigma_v = 1.1(n_3/13)^{\gamma/(2\gamma-2)}\,\mathrm{km\,s^{-1}} \qquad \rightarrow 2.43\, n_3^{-0.31}\,\mathrm{km\,s^{-1}} \quad ,$$

$$M = 230(n_3/13)^{(2\gamma+1)/(2\gamma-2)}\, M_\odot \qquad \rightarrow 8940\, n_3^{-1.42}\, M_\odot \quad ,$$

$$A_V = 21(n_3/13)^{(2\gamma-1)/(2\gamma-2)}\,\mathrm{mag} \qquad \rightarrow 13\, n_3^{0.19}\,\mathrm{mag} \quad ,$$

# The Fractal Structure of the Molecular Clouds

- Self-similarity of Clouds

  - The molecular interstellar medium is very clumpy and fragmented. Its hierarchical structure can well be described by a fractal, because of its self-similarity.

  - It has no characteristic scale. Fractals by definition are self-similar ensembles, that have a non-integer, i.e., fractional dimension.

  - ***The self-similar structures in the ISM extends over 6 orders of magnitude in scale, from about $10^{-4}$ to 100 pc.***

    ‣ These are not observed for the same molecular cloud only because of technical problems, lack of spatial resolution on one side, and difficulty of mapping too large areas on the other.

    ‣ The scaling relations all over the scales are however obtained by comparing various clouds observed with different resolutions.
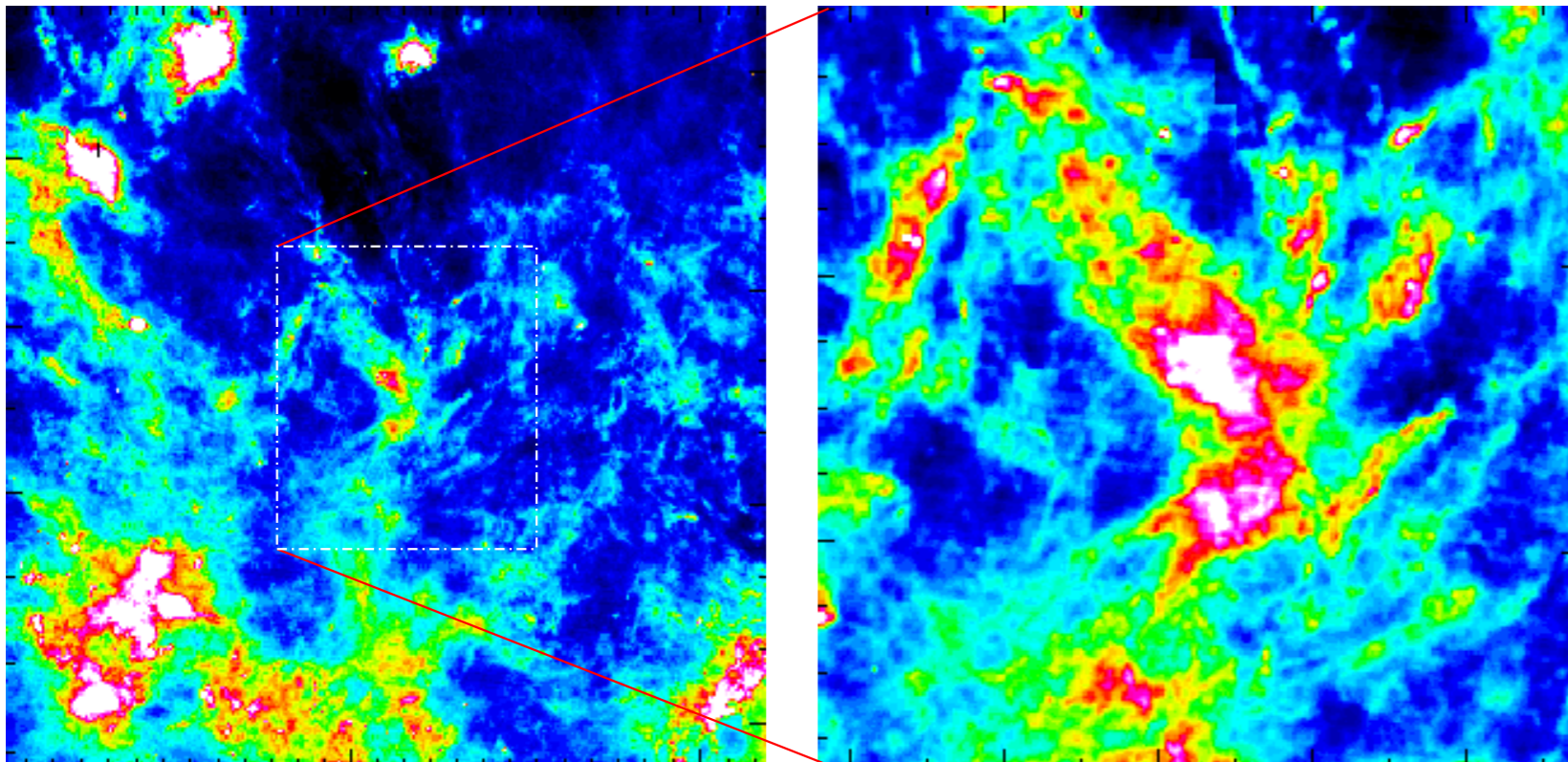


IRAS 100 μm map of molecular clouds towards the Taurus complex, located at about 100 pc from the Sun.
The square is ~ 4000 pc$^2$.

Fig 14, Chap 2, Blain, Combes, Draine [The Cold Universe]

# Excitation Temperature

- The excitation temperature for a given transition is defined as:

$$\frac{n_u}{n_\ell} = \frac{g_u}{g_\ell} e^{-h\nu_{ul}/kT_{\mathrm{exc}}}$$

   - For pure rotational transitions, the excitation temperature is often called the rotation temperature.

   - For vibrational transitions, it is called the vibrational temperature.

   - This nomenclature is analogous to the "spin temperature" defined for the H I 21-cm hyperfine transition.

# [Interstellar CO]

- Since the cold molecular hydrogen does not radiate (except the fluorescence UV line), the best tracer in galaxies is the most abundant molecule after $H_2$, i.e. the carbon monoxide CO. ***Much of what we know about molecular gas comes from observations of "tracer" molecules such as carbon monoxide (CO).***

- Fundamental frequencies

  - Vibrational frequency

    ‣ The fundamental vibrational frequency corresponds to to a wavelength:

      $$\lambda_0 = c/\nu_0 \approx 4.6\mu\mathrm{m}$$   This energy is ~50% of the energy in the $H_2$ fundamental frequency.

  - Rotational frequency:

    ‣ CO J=1-0, 2.60mm emission is the most important line used in studies of molecular gas.

      $$\lambda = 2.60\,\mathrm{mm} \rightarrow \nu = 115.3\,\mathrm{GHz} \rightarrow h\nu = 4.767 \times 10^{-4}\,\mathrm{eV} \rightarrow h\nu/k = 5.532\,\mathrm{K}$$

    ‣ This energy level is therefore perfectly fitted to probe the cold molecular clouds.

    ‣ The widely used CO lines (J = 1-0 at 2.6mm, J = 2-1 at 1.3 mm) are generally optically thick, for "standard" clouds of solar metallicity. This complicates the interpretation in terms of $H_2$ column densities and mass of the clouds.

- The line width $b$ that we measure for molecular line emission is often much broader than the thermal value $b \sim 0.1(T_{\mathrm{gas}}/20\,\mathrm{K})^{1/2}\,\mathrm{km\,s^{-1}}$ that we expect. *The large broadening is similar for molecules of different molecular mass*, suggesting that ***the broadening is due to turbulent motions within the cloud.***

- ## *Optical Depth & Velocity Structures*

  - Each individual molecular cloud is optically thick.

  - However, a giant molecular cloud is composed of many sub-structures, and there are many clouds along a line of sight. The "macroscopic" optical depth is in general not very large, due to velocity gradients: clouds do not hide each other at a given velocity, and therefore it is possible to "count" the clouds.

- ## *Isotopic Species*

  - Since the CO lines are optically thick (on average $\tau_{\mathrm{CO}} \sim 10$), it might be interesting to observe the much less abundant isotope $^{13}$CO.

  - At the solar neighborhood, the $^{12}$CO/$^{13}$CO abundance ratio is ~90, and in individual molecular clouds, it is frequent that the $^{13}$CO lines are optically thin.

    ‣ However, when maps of the two isotopes are compared at millimeter wavelengths for well studied clouds, it appears that the $^{13}$CO does not probe the entire extent of the clouds, but only the densest regions. This could be due to differences in excitation, self-shielding, or selective photo-dissociation.

  - The observed average ratio between integrated $^{12}$CO and $^{13}$CO intensities is of the order of 10.
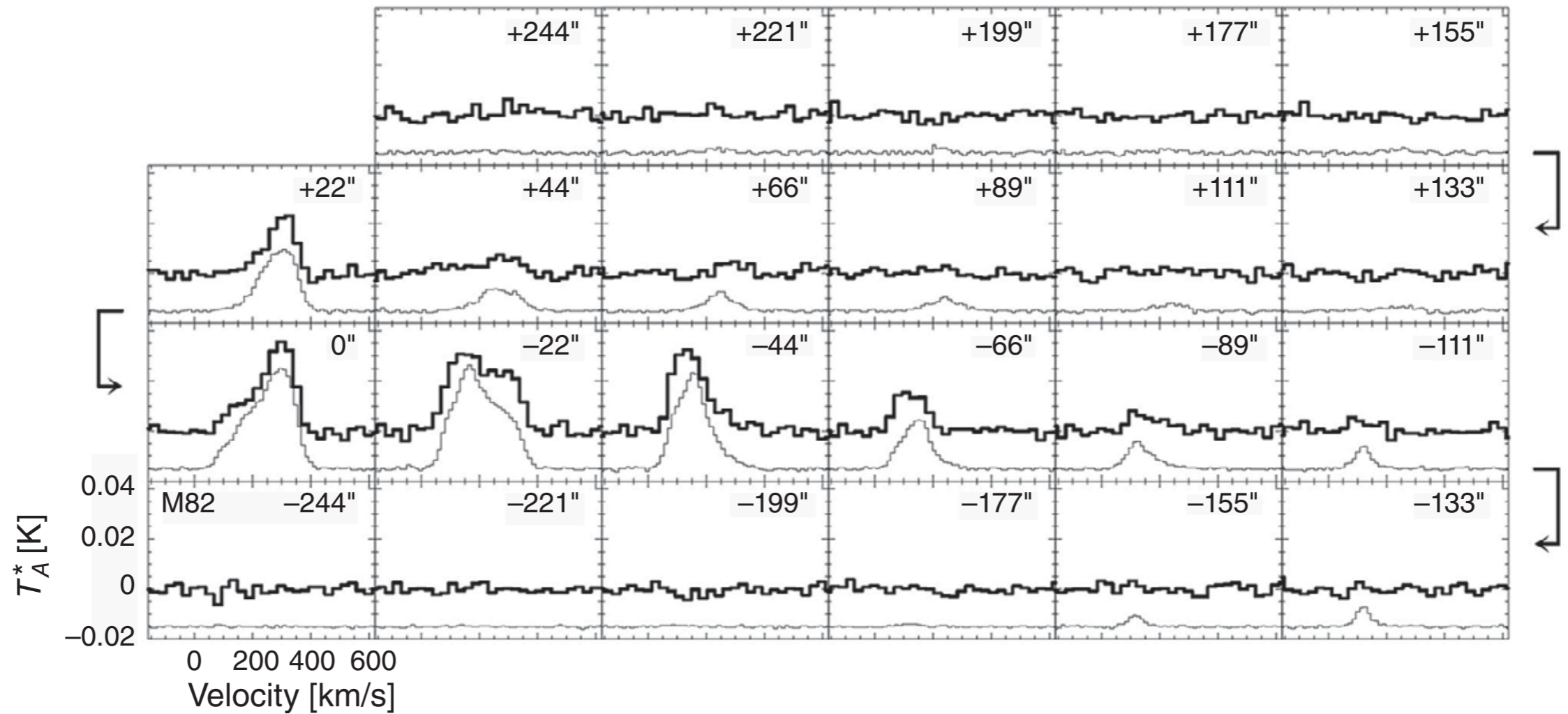
$^{13}$CO emission lines (thin) and $^{12}$CO emission lines divided by 10 (thick) for the $J = 1 \rightarrow 0$ transition, along the apparent major axis of the galaxy M82. At the $d \approx 3.5$ Mpc distance to M82, the 22 arcsec separation between the panels corresponds to ~370 pc.

[Paglione et al. 2001; Ryden]

# [Virial Theorem]

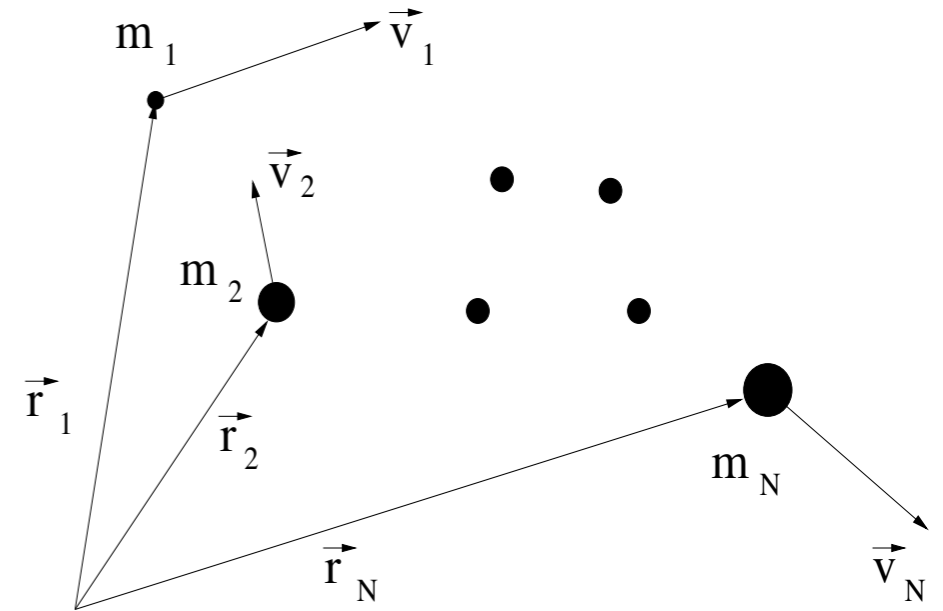- For a collection of *N* point particles, the total moment of inertia is given by

$$I = \sum_i m_i \left| \mathbf{r}_i \right|^2 = \sum_i m_i \mathbf{r}_i \cdot \mathbf{r}_i$$

- The time derivative of the moment of inertia is called the ***virial***:

$$Q = \frac{1}{2} \frac{dI}{dt} = \sum_i \mathbf{p}_i \cdot \mathbf{r}_i$$

Here, momentum vector:

$$\mathbf{p}_i = m_i \mathbf{v}_i \quad \left( = m_i \frac{d\mathbf{r}_i}{dt} \right)$$

Now take the time derivative of the viral

$$\frac{dQ}{dt} = \sum \mathbf{p}_i \cdot \mathbf{v}_i + \sum_i \frac{d\mathbf{p}_i}{dt} \cdot \mathbf{r}_i$$

$$= \sum_i m_i \mathbf{v}_i \cdot \mathbf{v}_i + \sum_i \mathbf{F}_i \cdot \mathbf{r}_i \quad \longleftarrow$$

Newton's second law:

$$\mathbf{F}_i = \frac{d\mathbf{p}_i}{dt} \quad \text{(the sum of all forces acting on particle } i\text{)}$$

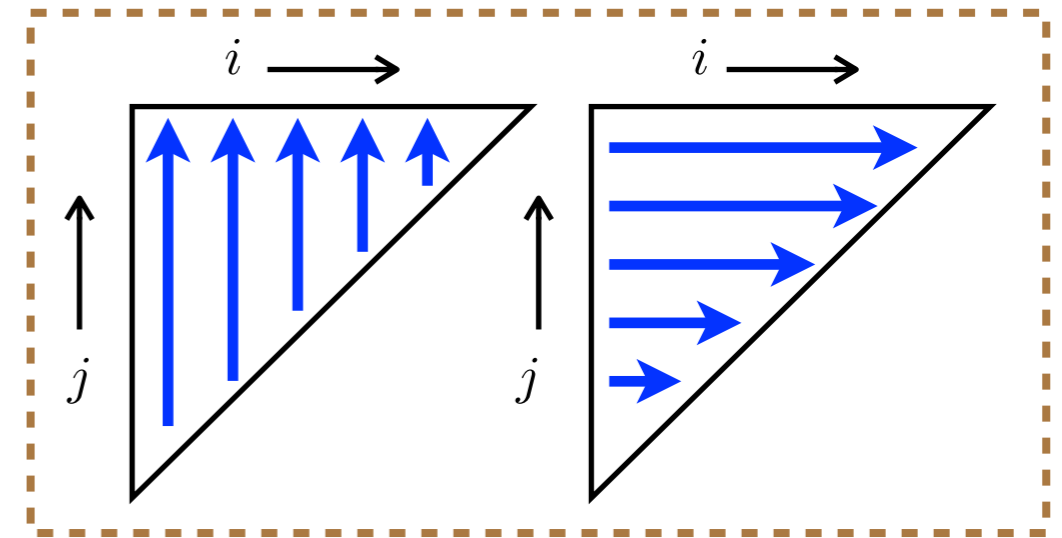The first term can be expressed in terms of the total kinetic energy of the system

$$\frac{dQ}{dt} = 2K + \sum_i \mathbf{F}_i \cdot \mathbf{r}_i \quad \left( \text{where } K = \sum_i \frac{1}{2} m_i \left| \mathbf{v}_i \right|^2 \right)$$

- The total force on particle $i$ is the sum of all the forces from the other particles $j$ in the system:

$$\mathbf{F}_i = \sum_{j \neq i} \mathbf{f}_{j \to i} \qquad \text{Here, } \mathbf{f}_{j \to i} \text{ is the force on particle } i \text{ from particle } j$$

Then,

$$\sum_{i=1}^{N} \mathbf{F}_i \cdot \mathbf{r}_i = \sum_{i=1}^{N} \sum_{j \neq i} \mathbf{f}_{j \to i} \cdot \mathbf{r}_i$$

$$= \sum_{i=1}^{N} \sum_{j < i} \mathbf{f}_{j \to i} \cdot \mathbf{r}_i + \sum_{i=1}^{N} \sum_{j > i} \mathbf{f}_{j \to i} \cdot \mathbf{r}_i$$

The last term can be rewritten as follows:



$$\sum_{i=1}^{N} \sum_{j > i} \mathbf{f}_{j \to i} \cdot \mathbf{r}_i = \sum_{j=1}^{N} \sum_{i < j} \mathbf{f}_{j \to i} \cdot \mathbf{r}_i \qquad \text{interchange the ordering of the sums.}$$

$$= \sum_{i=1}^{N} \sum_{j < i} \mathbf{f}_{i \to j} \cdot \mathbf{r}_j \qquad \text{interchange the name of the indices } i \text{ and } j.$$

$$= -\sum_{i=1}^{N} \sum_{j < i} \mathbf{f}_{j \to i} \cdot \mathbf{r}_j \qquad \text{Newton's third law: } \mathbf{f}_{i \to j} = -\mathbf{f}_{j \to i}$$

Hence,

$$\sum_{i=1}^{N} \mathbf{F}_i \cdot \mathbf{r}_i = \sum_{i=1}^{N} \sum_{j < i} \mathbf{f}_{j \to i} \cdot (\mathbf{r}_i - \mathbf{r}_j)$$

- Now, consider the gravitational force:

$$\mathbf{f}_{j\to i} = \frac{Gm_im_j}{r_{ij}^3}\left(\mathbf{r}_j - \mathbf{r}_i\right) \qquad\longrightarrow\qquad \sum_{i=1}^{N}\mathbf{F}_i\cdot\mathbf{r}_i = -\sum_{i=1}^{N}\sum_{j<i}\frac{Gm_im_j}{r_{ij}}$$

$$\text{where } r_{ij} = |\mathbf{r}_j - \mathbf{r}_i|$$

Note that the gravitational potential energy between particle $i$ and $j$ is given by $U_{ij} = -\dfrac{Gm_im_j}{r_{ij}}$.

$$\sum_{i=1}^{N}\mathbf{F}_i\cdot\mathbf{r}_i = \sum_{i=1}^{N}\sum_{j<i}U_{ij} = U \qquad \text{=> total potential energy of the system}$$

The total potential energy of the system is the sum of the potential energy between all possible pairs of particles (note that one pair of particle should be counted only once, this is why there is a $j < i$ in the second sum).

- We finally obtain the following. Now we take the mean value of the derivative of the virial over a long period of time:

$$\frac{dQ}{dt} = 2K + U \qquad\longrightarrow\qquad \left\langle\frac{dQ}{dt}\right\rangle = 2\left\langle K\right\rangle + \left\langle U\right\rangle$$

- If ***the system is bounded and the particles have finite momentum***, the average value will go to zero and we obtain the virial theorem:

$$\left\langle\frac{dQ}{dt}\right\rangle = \lim_{T\to\infty}\frac{Q(T) - Q(0)}{T} = 0 \qquad\longrightarrow\qquad 2\left\langle K\right\rangle + \left\langle U\right\rangle = 0 \qquad \begin{array}{c}\langle\rangle \text{ denotes both the ensemble average}\\ \text{and time average.}\end{array}$$

***Ergodic hypothesis***: Averaging system variables over a long time period is equal to averaging them over the ensemble.

$$\lim_{T\to\infty}\frac{1}{T}\int_0^T dt \to \lim_{N\to} \frac{1}{N}\sum_{i=1}^{N} \qquad \begin{array}{l}\text{If a bound system has a huge number of particles, it is equivalent to seeing}\\ \text{the system over a long period of time.}\end{array}$$

# Virial Mass Estimate

- A fundamental property is that GMCs are gravitationally bound and in viral equilibrium.

  - Their masses can then be estimated using line widths as a measure of the could velocities, following the arguments of Solomon et al.

  - The virial theorem provides a general equation that relates the average over time of the total kinetic energy of a stable, self-gravitating system of discrete particles, with the total potential energy of the system.

$$2 \langle K \rangle + \langle U \rangle = 0$$

  - For a uniform density sphere with a mass M and radius R, the gravitational potential energy is

$$U = -\frac{3}{5} \frac{GM^2}{R}$$

$$U = -\int_0^R \frac{GM_r dM_r}{r}$$

$$= -\int_0^R \frac{G}{r} \left( \frac{4\pi}{3} r^3 \rho \right) 4\pi r^2 \rho dr$$

$$= -\frac{(4\pi)^2}{3 \times 5} G\rho^2 R^5 = -\frac{3}{5} \frac{GM^2}{R}$$
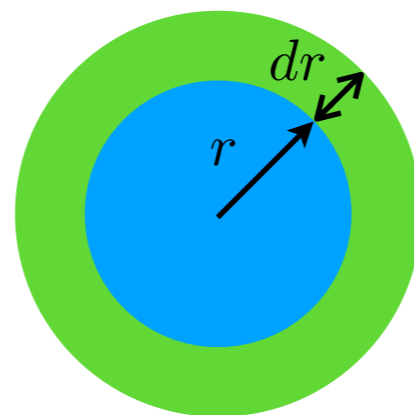
Density $\rho = \dfrac{M}{(4\pi/3)R^3}$

Mass within a radius $r$

$$M_r = \int_0^r \rho(4\pi r'^2 dr') = \frac{4\pi}{3} r^3 \rho$$

Mass between a shell $(r, r+dr)$

$$dM_r = \rho(4\pi r^2 dr)$$

- If the cloud is in equilibrium, with self-gravity being balanced by turbulent pressure, the virial theorem states that the turbulent velocity, in one dimension, to be

$$\langle K \rangle = \sum_i \frac{3}{2} m_i \left\langle v_i^2 \right\rangle = \frac{3}{2} \sum_i m_i \sigma_v^2 = \frac{3}{2} M \sigma_v^2$$

Here, $\sigma_v$ is the rms velocity dispersion.

$$2 \langle K \rangle + \langle U \rangle = 0 \quad \rightarrow \quad \sigma_v^2 = \frac{1}{5} \frac{GM}{R}$$

- Therefore, we obtain the total mass of the self-gravitation cloud in terms of the line width (broadening parameter):
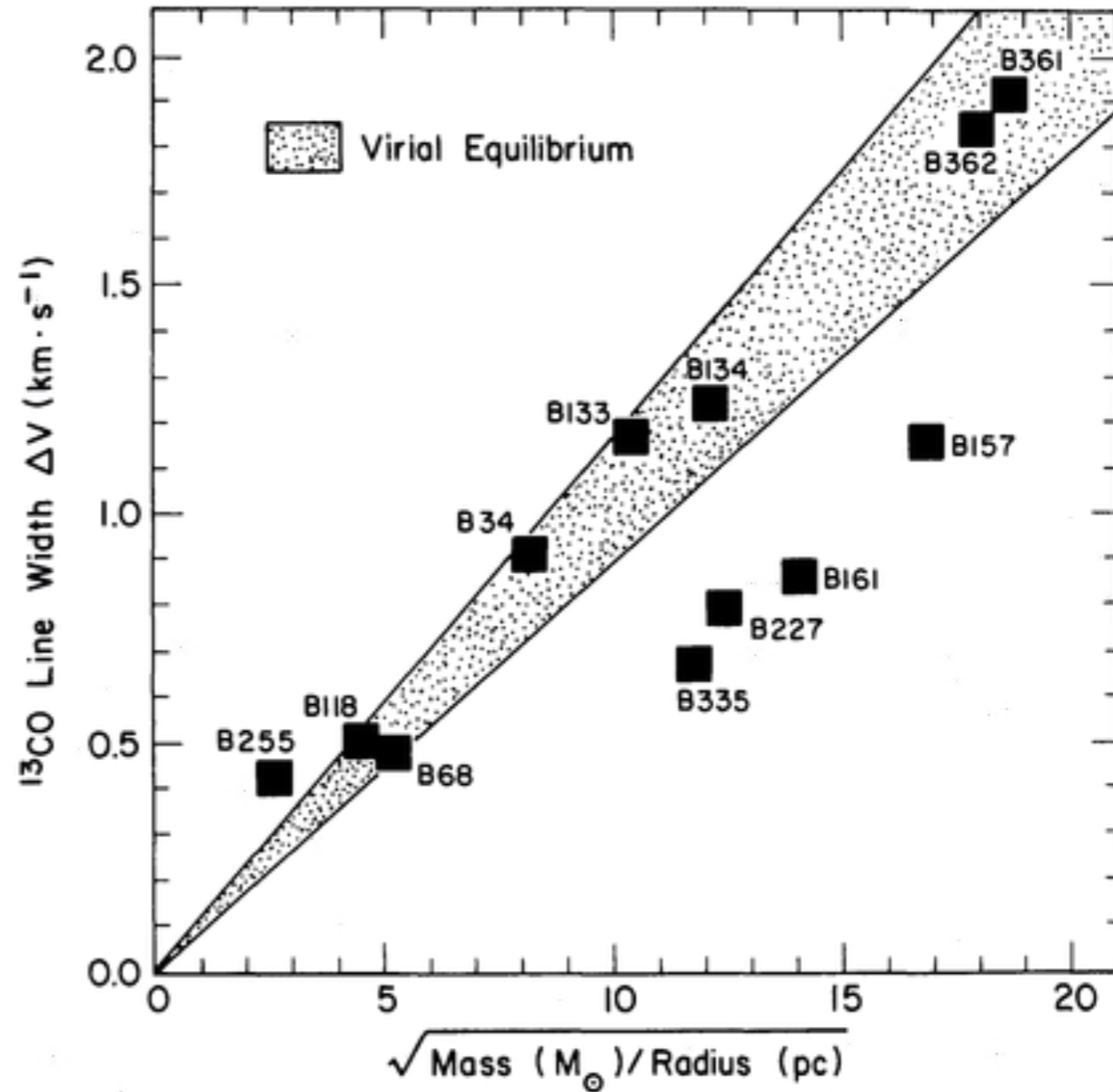
virial mass:
$$M = \frac{5b^2 R}{2G} \approx 600 \, M_\odot \left( \frac{b}{1 \, \mathrm{km\,s^{-1}}} \right)^2 \left( \frac{R}{1 \, \mathrm{pc}} \right)$$

Here, $b = \sqrt{2} \sigma_v$

- Note that the virial theorem for a uniform density clouds indicates that the following size-linewidth correlation if the density is constant. But, it appears that the density is not a constant, but controlled by turbulence.

$$b^2 = \frac{2}{5} \frac{GM}{R} = \frac{8\pi}{15} G\rho R^2 \quad \rightarrow \quad b = \left( \frac{8\pi}{15} G\rho \right)^{1/2} R$$

- The *line width - (mass/radius) correlation*:

$$b = \left(\frac{2G}{5}\right)^{1/2} \left(\frac{M}{R}\right)^{1/2}$$



The [13]CO line width versus (mass/radius)[1/2] for globules with $T < 10$K.

Fig 3, Leung et al. (1982, ApJ, 262, 583)

- The ***Mass - CO luminosity correlation***

$$L_{\text{CO}} \approx M \left( \frac{6\pi}{20} G \right)^{1/2} \frac{T_{\text{CO}}}{\sqrt{\rho}}$$

  - Let $I_{\text{CO}}$ the CO brightness temperature integrated over the line profile:

$$I_{\text{CO}} \equiv \int T_{\text{CO}} dv \approx T_{\text{CO}} b \quad (b \approx \Delta v)$$

  - The CO luminosity of a cloud is:

$$L_{\text{CO}} \equiv D^2 \int I_{\text{CO}} d\Omega \approx \pi R^2 T_{\text{CO}} b$$

$$= \sqrt{\frac{2\pi^2}{5} G M R^3} = \sqrt{\frac{6\pi}{20} G} \frac{T_{\text{CO}}}{\sqrt{\rho}} M$$



Here, *D* = distance, and virial condition: $b \approx \sqrt{\frac{2}{5} \frac{GM}{R}}$

  - To the extend that the ratio $\sqrt{\rho}/T_{\text{CO}}$ does not vary in the mean from cloud to cloud, this indicates that the total CO luminosity is directly proportional to the total mass of molecular clouds. However, in reality, the power-law slope is ~ 0.76.

  - ***This correlation supports the fundamental assumption that GMCs are in virial equilibrium.***
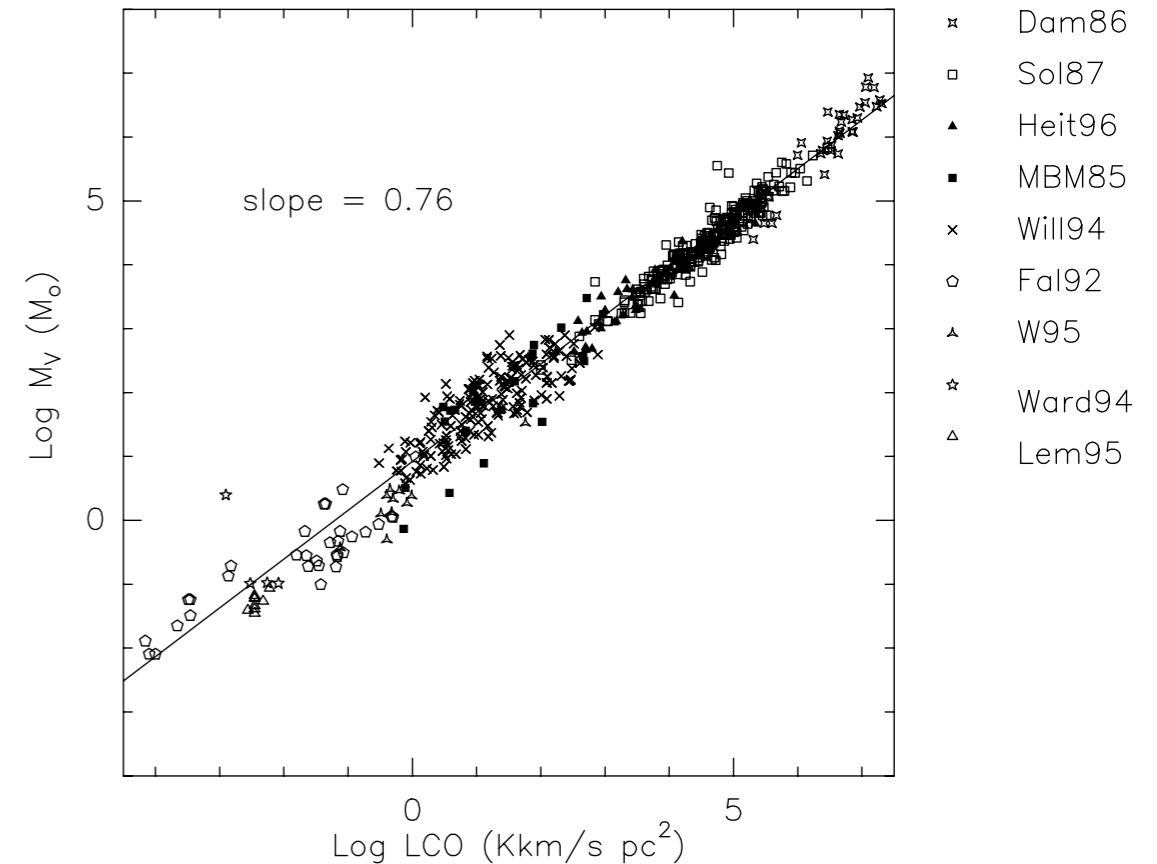
Virial mass versus CO luminosity relation taken from various sources:

Fig 4, Chap 2, Blain, Combes, & Draine [The cold Universe]